Asymptotic dynamics in scalar field theory: Anomalous relaxation

D. Boyanovsky,[1] C. Destri,[2] H. J. de Vega,[3] R. Holman,[4] and J. Salgado[3]
[1]*Department of Physics and Astronomy, University of Pittsburgh, Pittsburgh, Pennsylvania 15260*
[2]*Dipartimento di Fisica, Università di Milano and INFN, sezione di Milano, Via Celoria 16, 20133 Milano, Italy*
[3]*LPTHE, Université Pierre et Marie Curie (Paris VI) et Denis Diderot (Paris VII), Tour 16, 1er. étage, 4, Place Jussieu 75252 Paris, Cedex 05, France*
[4]*Department of Physics, Carnegie Mellon University, Pittsburgh, Pennsylvania 15213*
(Received 19 November 1997; published 3 June 1998)

We analyze the dynamics of dissipation and relaxation in the unbroken and broken symmetry phases of scalar theory in the *nonlinear* regime for large initial energy densities, and after *linear* unstabilities (parametric or spinodal) are shut off by the quantum back reaction. A new time scale emerges that separates the linear from the non-linear regimes. This scale is non-perturbative in the coupling and initial amplitude. The non-perturbative evolution is studied within the context of the $O(N)$ vector model in the large N limit. A combination of numerical analysis and the implementation of a dynamical renormalization group resummation via multi-time-scale analysis reveals the presence of unstable bands in the nonlinear regime. These are associated with *power law* growth of quantum fluctuations, that result in power law relaxation and dissipation with *non-universal and non-perturbative dynamical anomalous exponents*. We find that there is substantial particle production during this non-linear evolution which is of the same order as that in the linear regime and results in a non-perturbative distribution. The expectation value of the scalar field vanishes asymptotically transferring all of the initial energy into produced particles via the non-linear resonances in the unbroken symmetry phase. The effective mass squared for the quantum modes tends asymptotically to a constant plus oscillating $\mathcal{O}(1/t)$ terms. This slow approach to asymptotia causes the power behavior of the modes which become free harmonic modes for late enough time. We derive a simple expression for the equation of state for the fluid of produced particles that interpolates between radiation-type and dust-type equations according to the initial value of the order parameter for unbroken symmetry. For broken symmetry the produced particles are asymptotically massless Goldstone bosons with an ultrarelativistic equation of state. We find the onset of a novel form of dynamical Bose condensation in the collisionless regime in the absence of thermalization. [S0556-2821(98)04910-8]

PACS number(s): 11.10.Jj, 11.15.Pg, 98.80.Cq

I. INTRODUCTION AND MOTIVATION

The next generation of high luminosity heavy ion colliders at Brookhaven and CERN will offer the possibility of probing the dynamics of states of high energy density and possibly strongly out of equilibrium. The energy densities attained for central collisions at central rapidity will hopefully allow us to study the quark-gluon plasma and also the chiral phase transition in a situation that parallels that achieved in the very early stages of the Universe [1–5]. Dynamical phenomena and nonequilibrium and collective effects are expected to take place on time scales of a few tens of fm/c and length scales of a few fermis.

This unparalleled short time and length scale regime for dynamical phenomena, soon to be probed experimentally, has sparked a considerable effort to study the *dynamics* of strongly out of equilibrium situations within the realm of quantum field theory.

The usual semi-phenomenological framework to study the dynamics is based on the transport approach in terms of single (quasi-)particle distribution functions with collisional relaxation [6–8]. The best known dynamical processes of relaxation are those of (few body) collisions and dephasing processes akin to Landau damping [7–16]. Our understanding of these relaxational processes is usually based on perturbative expansions, linearized approximations or small departures from equilibrium. The validity of these coarse grained descriptions of relaxational dynamics within the realm of high energy and high density regimes in quantum field theory is not clear and a closer scrutiny of relaxational phenomena is warranted.

Whereas equilibrium phenomena are fairly well understood and there are a variety of tools to study perturbative and non-perturbative aspects, strongly out of equilibrium phenomena are not well understood and require different techniques.

Our goal is to deal with the out of equilibrium evolution for *large* energy densities in field theory, that is, a large number of particles per volume m^{-3}, where m is the typical mass scale in the theory. The most familiar techniques of field theory, based on the S-matrix formulation of transition amplitudes and perturbation theory, apply in the opposite limit of low energy density, and since they only provide information on $in \rightarrow out$ matrix elements, are unsuitable for calculations of time dependent expectation values.

Recently non-perturbative approaches to study particle production [17], dynamics of phase transitions [17,18] and novel forms of dissipation [20] have emerged that provide a promising framework to study the dynamics for large energy densities like in heavy ion collisions.

Similar tools are also necessary to describe consistently the dynamical processes in the early Universe [20]. In par-

ticular it has been recognized that novel phenomena associated with parametric amplification of quantum fluctuations can play an important role in the process of reheating and thermalization [19,20–23]. It must be noticed that the dynamics in cosmological spacetimes is dramatically different to the dynamics in Minkowski spacetime. Both in fixed Friedmann-Robertson-Walker (FRW) [36] and de Sitter [35] backgrounds and in a dynamical geometry [37] the dynamical evolution is qualitatively and quantitatively different from the Minkowski case considered in the present paper.

Our program to study the dynamical aspects of relaxation out of equilibrium both in the linear and non-linear regime has revealed new features of relaxation in the collisionless regime in scalar field theories [20,24]. Recent investigations of scalar field theories in the non-linear regime, including self-consistently the effects of quantum back reaction in an energy conserving and renormalizable framework, have pointed out a wealth of interesting non-perturbative phenomena both in the broken and unbroken symmetry phases [20]. These new phenomena are a consequence of the non-equilibrium evolution of an initial state of large energy density which results in copious particle production leading to a non-thermal and non-perturbative distribution of particles. Our studies have focused on the situation in which the *amplitude* of the expectation value of the scalar field is non-perturbatively large, $A \approx \sqrt{\lambda}\langle\Phi\rangle/m \approx \mathcal{O}(1)$ (m is the mass of the scalar field and λ the self-coupling) and most of the energy of the initial state is stored in the ''zero mode,'' i.e. the (translational invariant) expectation value of the scalar field Φ. Under these circumstances the initial energy density $\varepsilon \approx m^4/\lambda$. During the dynamical evolution the energy initially stored in one (or few) modes of the field is transferred to other modes, resulting in copious particle production initially either by parametric amplification of quantum fluctuations in the unbroken symmetry phase or spinodal instabilities in the broken symmetry phase. This mechanism of energy dissipation and particle production results in a number of produced particles per unit volume, $\mathcal{N} \propto m^3/\lambda$, which for weak coupling is non-perturbatively large [20]. We call this first stage dominated either by parametric or spinodal unstabilities the ''linear regime.''

We recognized [20] a new *dynamical* time scale t_1 where the linear regime ends. By the time t_1 the effects of the quantum fluctuation on the dynamical evolution become of the same order as the classical contribution given by the evolution of the expectation value of the field. The ''non-linear regime'' starts by the time t_1. In the case of broken symmetry, this time scale corresponds to the spinodal scale at which the back reaction of quantum fluctuations shut off the spinodal instabilities. At this scale non-perturbative physics sets in and the non-linearities of the full quantum theory determine the evolution. This time scale t_1, which we call the *non-linear time*, is a non-universal feature of the dynamics and depends strongly on the initial state and non-perturbatively on the coupling, as $t_1 \propto \log[\lambda^{-1}]$ for weak coupling [20].

The purpose of this paper is to carefully analyze the *non-linear* dynamics of relaxation after the time t_1 in a weakly coupled scalar field theory within a non-perturbative self-consistent scheme. We focus on the asymptotic time regime both in the unbroken and broken symmetry states. Here we provide refined numerical analysis of the non-equilibrium evolution that reveals the onset of widely separated relaxational time scales. We use a *dynamical renormalization group* implemented via a multitime scale analysis to provide an analytic description of the asymptotic dynamics and establish that relaxation occurs via power laws with anomalous dynamical exponents.

The main results of this article can be summarized as follows:

The hierarchy of separated time scales allows us to implement a dynamical renormalization group resummation via the method of multitime scale analysis. The novel result that emerges from this combination of numerical and dynamical renormalization group analysis is the presence of *non-linear resonances* that lead to asymptotic relaxation described by *non-universal power laws*. These power laws are determined by *dynamical anomalous exponents* which depend non-perturbatively on the coupling.

The effective mass felt by the quantum field modes in high energy density situations varies with time and depends on the fields themselves, reflecting the nonlinear character of the dynamics. Both for broken and unbroken symmetry the effective mass tends asymptotically to a constant. This constant is non-zero and depends on the initial state for unbroken symmetry. For broken symmetry, the effective mass tends to zero, corresponding to Goldstone bosons. In both cases the effective mass approaches its $t=\infty$ value as $1/t$ times oscillating functions.

The fact that the effective mass tends asymptotically to a constant implies that the modes become effectively *free*. Non-resonant modes oscillate harmonically for times $t > t_1$. Resonant modes change from non-universal power behavior to oscillatory behavior at a time that depends on the wave number of the mode. Only the modes in the borders of the band resonate indefinitely.

In the unbroken symmetry case, we find that the expectation value relaxes to zero asymptotically with a non-universal power law. The initial energy density which is non-perturbatively large goes completely into the production of massive particles. The asymptotic particle distribution is localized within a band determined by the initial conditions with non-perturbatively large amplitude $\sim 1/\sqrt{\lambda}$ which could be described as a ''semiclassical condensate'' in the unbroken phase.

The particle distribution in the condensate is nontrivial. We establish sum rules that yield explicit values for integrals over such an asymptotic distribution. We derive in this way the asymptotic equation of state. For unbroken symmetry, it interpolates between dust and radiation according to the initial field amplitude.

In the broken symmetry phase when the initial expectation value of the scalar field (order parameter) is close to the false vacuum (at the origin) we similarly find the onset of non-linear resonances at times larger than the non-linear (spinodal) time t_1. The expectation value of the order parameter approaches for late times a nonzero limit that depends on the initial conditions.

The effective time dependent mass vanishes as $1/t$, resulting in the asymptotic states being Goldstone bosons. We also find a hierarchy of time scales of which $t_1 \propto \ln[\lambda^{-1}]$ is the first and another longer time scale $t_2 \propto 1/\sqrt{\lambda}$. As a conse-

quence of the non-linear resonances the particle distribution becomes localized for $t>t_1$ at very low momentum, resulting again in a ''semiclassical condensate'' with non-perturbatively large amplitude $\sim 1/\sqrt{\lambda}$. Asymptotically the equation of state is that of radiation although the particle distribution (Goldstone bosons) is non-thermal.

For even larger time scales, $t\sim\sqrt{V}$ (where V stands for the volume of the system), we find for broken symmetry a novel form of Bose condensation in the collisionless regime that results from a linear growth in time of homogeneous quantum fluctuations.

The article is organized as follows: In Sec. II we briefly summarize the nature of the approximations, the non-equilibrium framework and some of the previous results for the benefit of the reader and for coherence. In Sec. III we study the unbroken symmetry case and distinguish the linear regime of parametric amplification $t<t_1$ from the non-linear regime ($t>t_1$) in which the back reaction of quantum fluctuations dominates the evolution. In Sec. IV we study the latter regime in the unbroken symmetry case and we find that particle production continues beyond $t>t_1$ and non-linear resonances develop, leading to power law relaxation. We provide a full numerical analysis and implement a renormalization group resummation of secular terms via a multi-time-scale approach. Asymptotic sum rules and the equation of state are discussed in detail. In Sec. V we study the dynamics in the broken symmetry phase, establishing a difference between the early and intermediate scales dominated by spinodal instabilities and the asymptotically large time scale dominated by non-linear resonances leading to power law relaxation. We provide a numerical analysis as well as arguments based on multitime scale resummation. We find a novel form of Bose condensation with a quadratic time dependence for the formation of an homogeneous condensate.

Conclusions and further questions are summarized at the end of the article.

II. PRELIMINARIES

As our previous studies of scalar field theory have revealed [20], there are two very important parameters that influence the quantum dynamics: the strength of the coupling constant λ and the initial energy density in units of the scalar field mass m. If in the initial state most of the energy is stored in a few modes, the energy density is determined by the amplitude of the expectation value of those modes, $A\approx\sqrt{\lambda}\langle\Phi\rangle/m$. The value of this field amplitude determines the regime of applicability of perturbation theory methods. Usual S-matrix theory treatments (in terms of a perturbative expansion) are valid in the small amplitude regime $A\ll 1$ even for high energies. However, when the initial state has a large energy *density* perturbative methods are invalid.

We shall be concerned here with the *non-perturbative* regime in which $A=\sqrt{\lambda}\langle\Phi\rangle/m\simeq\mathcal{O}(1)$. It is important to point out that for a large field amplitude, even for very weakly coupled theories non-linear effects will be important and must be treated non-perturbatively. This is the case under consideration. Having recognized the non-perturbative nature of the problem for large amplitudes we must invoke a non-perturbative, consistent calculational scheme which respects the symmetries (continuous global symmetries and energy-momentum conservation), is renormalizable and lends itself to a numerical treatment.

We are thus led to consider the $O(N)$ vector model with a quartic self-interaction [20] and the scalar field in the vector representation of $O(N)$.

The action and Lagrangian density are given by

$$S=\int d^4x\mathcal{L},$$

$$\mathcal{L}=\frac{1}{2}[\partial_\mu\vec{\Phi}(x)]^2-V(\vec{\Phi}(x)),$$

$$V(\vec{\Phi})=\frac{\lambda}{8N}\left(\vec{\Phi}^2+\frac{2Nm^2}{\lambda}\right)^2-\frac{Nm^4}{2\lambda}. \tag{2.1}$$

The canonical momentum conjugate to $\vec{\Phi}(x)$ is

$$\vec{\Pi}(x)=\dot{\vec{\Phi}}(x), \tag{2.2}$$

and the Hamiltonian is given by

$$H(t)=\int d^3x\left\{\frac{1}{2}\vec{\Pi}^2(x)+\frac{1}{2}[\nabla\vec{\Phi}(x)]^2+V(\vec{\Phi})\right\}. \tag{2.3}$$

The calculation of expectation values requires the study of a density matrix, whether or not the initial state is pure or mixed. Its time evolution in the Schrödinger picture is determined by the quantum Liouville equation

$$i\frac{\partial\hat{\rho}}{\partial t}=[H,\hat{\rho}]. \tag{2.4}$$

The expectation value of any physical magnitude $\mathcal{A}$ is given as usual by

$$\langle\mathcal{A}\rangle(t)=\mathrm{Tr}[\hat{\rho}(t)\mathcal{A}]. \tag{2.5}$$

The time evolution of all physical magnitudes is unitary as we see from Eq. (2.4).

In the present case we will restrict ourselves to a translationally invariant situation; i.e., the density matrix commutes with the total momentum operator. In this case the order parameter $\langle\vec{\Phi}(\vec{x},t)\rangle$ will be independent of the spatial coordinates $\vec{x}$ and only depends on time.

We write the field $\vec{\Phi}$ as $\vec{\Phi}=(\sigma,\vec{\pi})$ where $\vec{\pi}$ represents the $N-1$ ''pions,'' and choose the coupling λ to remain fixed in the large N limit. In what follows, we will consider two different cases of the potential (2.1), $V(\sigma,\vec{\pi})$, with ($m^2<0$) or without ($m^2>0$) symmetry breaking.

We can decompose the field σ into its expectation value and fluctuations $\chi(\vec{x},t)$ about it:

$$\sigma(\vec{x},t)=\Phi(t)\sqrt{N}+\chi(\vec{x},t), \tag{2.6}$$

with $\Phi(t)$ being a c-number of order 1 in the $N\to\infty$ limit and χ an operator.

To leading order the large N-limit is implemented by considering a Hartree-like factorization (neglecting $1/N$ terms)

and assuming $O(N-1)$ invariance by writing

$$\vec{\pi}(\vec{x},t) = \Psi(\vec{x},t)\overbrace{(1,1,\cdots,1)}^{N-1} \tag{2.7}$$

where $\Psi(\vec{x},t)$ is a quantum operator [20]. Alternatively the large N expansion is systematically implemented by introducing an auxiliary field [17]. To leading order the two methods are equivalent.

The generating functional of real time non-equilibrium Green's functions can be written in terms of a path integral along a complex contour in time, corresponding to forward and backward time evolution, and if the initial density matrix describes a state of local thermodynamic equilibrium at finite temperature, a branch down the imaginary time axis. This requires doubling the number of fields which now carry a label $\pm$ corresponding to forward $(+)$ and backward $(-)$ time evolution [25,26].

We shall not rederive here the field evolution equations for translationally invariant quantum states; the reader is referred to the literature. (See Refs. [25–27].) In the leading order in the large N approximation the theory becomes Gaussian at the expense of a self-consistent condition [17,20,27]; this in turn entails that the Heisenberg field operator $\Psi(\vec{x},t)$ can be written as

$$\Psi(\vec{x},t) = \int \frac{d^3k}{(2\pi)^3}\frac{1}{\sqrt{2}}[a_{\vec{k}} f_k(t) e^{i\vec{k}\cdot\vec{x}} + a^\dagger_{\vec{k}} f^*_k(t) e^{-i\vec{k}\cdot\vec{x}}], \tag{2.8}$$

where a_k, $a^\dagger_k$ are the canonical creation and annihilation operators, and the mode functions $f_k(t)$ are solutions of the Heisenberg equations of motion [17,20,27] to be specified below for each case.

Our choice of initial conditions on the density matrix is that of the vacuum for the instantaneous modes of the Hamiltonian at the initial time [20,27]. Therefore we choose the initial conditions on the mode functions to represent positive energy particle states of the instantaneous Hamiltonian at $t=0$, which is taken to be the initial time. That is,

$$f_k(0) = \frac{1}{\sqrt{W_k}}, \quad \dot{f}_k(0) = -i\sqrt{W_k}, \quad W_k = \sqrt{k^2 + M_0^2}, \tag{2.9}$$

where the mass M_0 determines the frequencies $\omega_k(0)$ and will be defined explicitly later as a function of $\Phi(0)$ [see Eqs. (3.5) and (5.4)].

With these boundary conditions, the mode functions $f_k(0)$ correspond to positive frequency modes (particles) of the instantaneous quadratic Hamiltonian for oscillators of mass M_0.

We point out that the behavior of the system depends mildly on the initial conditions on the mode functions as we have found by varying Eqs. (2.9) within a wide range. In particular, the various types of linear and nonlinear resonances are independent of these initial conditions [20,27].

It proves convenient to introduce the following dimensionless quantities:

$$\tau = |m|t, \quad q = \frac{k}{|m|}, \quad \Omega_q = \frac{W_k}{|m|}, \tag{2.10}$$

$$\eta^2(\tau) = \frac{\lambda}{2|m|^2}\Phi^2(t), \tag{2.11}$$

$$g\Sigma(\tau) = \frac{\lambda}{2|m|^2}[\langle\Psi^2(t)\rangle_R - \langle\Psi^2(0)\rangle_R] \quad (\Sigma(0)=0), \tag{2.12}$$

$$g = \frac{\lambda}{8\pi^2}, \quad \varphi_q(\tau) \equiv \sqrt{|m|} f_k(t). \tag{2.13}$$

Here $\langle\Psi^2(t)\rangle_R$ stands for the renormalized composite operator [see Eq. (3.7) for an explicit expression].

In the $N=\infty$ limit the field $\chi(\vec{x},t)$ decouples and does not contribute to the equations of motion of either the expectation value or the transverse fluctuation modes.

III. UNBROKEN SYMMETRY

A. Evolution equations in the large N limit

In this case $M_R^2 = |M_R|^2$, and in terms of the dimensionless variables introduced above the renormalized equations of motion are found to be (see Refs. [20,27])

$$\ddot{\eta} + \eta + \eta^3 + g\,\eta(\tau)\Sigma(\tau) = 0, \tag{3.1}$$

$$\left[\frac{d^2}{d\tau^2} + q^2 + 1 + \eta(\tau)^2 + g\Sigma(\tau)\right]\varphi_q(\tau) = 0, \tag{3.2}$$

$$\varphi_q(0) = \frac{1}{\sqrt{\Omega_q}}, \quad \dot{\varphi}_q(0) = -i\sqrt{\Omega_q},$$

$$\eta(0) = \eta_0, \quad \dot{\eta}(0) = 0. \tag{3.3}$$

Hence,

$$\mathcal{M}^2(\tau) \equiv 1 + \eta(\tau)^2 + g\Sigma(\tau) \tag{3.4}$$

plays the role of a (time dependent) effective mass squared.

As mentioned above, the choice of Ω_q determines the initial state. We will choose these such that at $t=0$ the quantum fluctuations are in the ground state of the oscillators at the initial time. Recalling that by definition $g\Sigma(0)=0$, we choose the dimensionless frequencies to be

$$\Omega_q = \sqrt{q^2 + 1 + \eta_0^2}. \tag{3.5}$$

The Wronskian of two solutions of Eq. (3.2) is given by

$$\mathcal{W}[\varphi_q, \overline{\varphi_q}] = 2i, \tag{3.6}$$

while $g\Sigma(\tau)$ is given by the self-consistent condition [20,27]

$$g\Sigma(\tau)=g\int_0^\infty q^2dq\left\{|\varphi_q(\tau)|^2-\frac{1}{\Omega_q}+\frac{\theta(q-1)}{2q^3}[-\eta_0^2+\eta^2(\tau)+g\Sigma(\tau)]\right\}. \quad (3.7)$$

We thus see that the effective mass at time τ contains all q-modes and the zero mode at the same time τ. The evolution equations are then nonlinear but local in time in the infinite N limit.

B. Particle number

Although the notion of particle number is ambiguous in a time dependent non-equilibrium situation, a suitable definition can be given with respect to some particular pointer state. We consider two particular definitions that are physically motivated and relevant as we will see later. The first corresponds to defining particles with respect to the initial Fock vacuum state, while the second corresponds to defining particles with respect to the instantaneous adiabatic vacuum state.

In the former case we write the spatial Fourier transform of the fluctuating field $\Psi(\vec{x},\tau)$ in Eq. (2.8) and its canonical momentum $\Pi(\vec{x},\tau)$ as

$$\psi_q(\tau)=\frac{1}{\sqrt{2}}[a_q\varphi_q(\tau)+a^\dagger_{-q}\varphi^*_q(\tau)]$$

$$\Pi_q(\tau)=\frac{1}{\sqrt{2}}[a_q\dot{\varphi}_q(\tau)+a^\dagger_{-q}\dot{\varphi}^*_q(\tau)]$$

with the *time independent* creation and annihilation operators, such that a_q annihilates the initial Fock vacuum state. Using the initial conditions on the mode functions, the Heisenberg field operators are written as

$$\psi_q(\tau)=\mathcal{U}^{-1}(\tau)\psi_q(0)\mathcal{U}(\tau)=\frac{1}{\sqrt{2\Omega_q}}[\tilde{a}_q(\tau)+\tilde{a}^\dagger_{-q}(\tau)]$$

$$\Pi_q(\tau)=\mathcal{U}^{-1}(\tau)\Pi_q(0)\mathcal{U}(\tau)=-i\sqrt{\frac{\Omega_q}{2}}[\tilde{a}_q(\tau)-\tilde{a}^\dagger_{-q}(\tau)]$$

$$\tilde{a}_q(\tau)=\mathcal{U}^{-1}(\tau)a_q\mathcal{U}(\tau)$$

with $\mathcal{U}(\tau)$ the time evolution operator with the boundary condition $\mathcal{U}(0)=1$. The Heisenberg operators $\tilde{a}_q(\tau)$, $\tilde{a}^\dagger_q(\tau)$ are related to $a_q, a^\dagger_q$ by a Bogoliubov (canonical) transformation (see Refs. [20,27] for details).

The particle number with respect to the initial Fock vacuum state is defined in term of the dimensionless variables introduced above as

$$N_q(\tau)=\langle\tilde{a}^\dagger_q(\tau)\tilde{a}_q(\tau)\rangle=\frac{1}{4}\left[\Omega_q|\varphi_q(\tau)|^2+\frac{|\dot{\varphi}_q(\tau)|^2}{\Omega_q}\right]-\frac{1}{2}. \quad (3.8)$$

We consider here zero initial temperature so the occupation number vanishes at $\tau=0$.

In order to define the particle number with respect to the adiabatic vacuum state we note that the mode equations (3.2), (5.2) are those of harmonic oscillators with time dependent squared frequencies

$$\omega_q^2(\tau)=q^2+1+\eta^2(\tau)+g\Sigma(\tau). \quad (3.9)$$

When the frequencies are real (as is the case for unbroken symmetry), the adiabatic modes can be introduced in the following manner:

$$\psi_q(\tau)=\frac{1}{\sqrt{2\,\omega_q(\tau)}}[\alpha_q(\tau)e^{-i\int_0^t\omega_q(\tau')d\tau'}+\alpha^\dagger_{-q}(\tau)e^{i\int_0^t\omega_q(\tau')d\tau'}] \quad (3.10)$$

$$\Pi_q(\tau)=-i\sqrt{\frac{\omega_q(\tau)}{2}}[\alpha_q(\tau)e^{-i\int_0^t\omega_q(\tau')d\tau'}-\alpha^\dagger_{-q}(\tau)e^{i\int_0^t\omega_q(\tau')d\tau'}] \quad (3.11)$$

where now $\alpha_q(\tau)$ is a canonical operator that annihilates the adiabatic vacuum state, and is related to a_q , $a^\dagger_q$ by a Bogoliubov transformation. This expansion diagonalizes the instantaneous Hamiltonian in terms of the canonical operators $\alpha_q(\tau)$, $\alpha^\dagger_q(\tau)$. The adiabatic particle number is given by

$$N^{ad}_q(\tau)=\langle\alpha^\dagger_q(\tau)\alpha_q(\tau)\rangle=\frac{1}{4}\left[\omega_q(\tau)|\varphi_q(\tau)|^2+\frac{|\dot{\varphi}_q(\tau)|^2}{\omega_q(\tau)}\right]-\frac{1}{2}. \quad (3.12)$$

These adiabatic modes and the corresponding adiabatic particle number have been used previously within the non-equilibrium context [17] and will be very useful in the analysis of the energy below. Both definitions coincide at $\tau=0$ because $\omega_q(0)=\Omega_q$. (For non-zero initial temperature see Refs. [20,27,17]).

The total number of produced particles $\mathcal{N}^{ad}(\tau)$ per volume $|M_R|^3$ is given by

$$\mathcal{N}^{ad}(\tau)\equiv\int\frac{d^3q}{(2\pi)^3}N^{ad}_q(\tau). \quad (3.13)$$

The asymptotic behavior of the mode functions ensures that this integral converges [20,27].

C. Early time evolution: Parametric resonance

Let us briefly review the dynamics in the weak coupling regime and for times small enough so that the quantum fluctuations, i.e. $g\Sigma(\tau)$, are not large compared to the ''tree level'' quantities. As shown in Refs. [20,27], the back-reaction term $g\Sigma(\tau)$ is small for small g during an interval say $0\leqslant\tau<\tau_1$. This time τ_1, to be determined below, will be called the nonlinear time and it determines the time scale when the back-reaction effects and therefore the quantum fluctuations and non-linearities become important.

During the interval of time in which the back-reaction term $g\Sigma(\tau)$ can be neglected Eq. (3.1) reduces to the classical equation of motion (in dimensionless variables)

$$\ddot{\eta}+\eta+\eta^3=0. \tag{3.14}$$

The solution of this equation with the initial conditions (3.3) can be written in terms of elliptic functions with the result

$$\eta(\tau)=\eta_0 \mathrm{cn}(\tau\sqrt{1+\eta_0^2},k), \quad k=\frac{\eta_0}{\sqrt{2(1+\eta_0^2)}}, \tag{3.15}$$

where cn stands for the Jacobi cosine. Notice that $\eta(\tau)$ has period $4\omega\equiv 4K(k)/\sqrt{1+\eta_0^2}$, where $K(k)$ is the complete elliptic integral of first kind.

Inserting this form for $\eta(\tau)$ in Eq. (3.2) and neglecting $g\Sigma(\tau)$ yields

$$\left[\frac{d^2}{d\tau^2}+q^2+1+\eta_0^2 \mathrm{cn}^2(\tau\sqrt{1+\eta_0^2},k)\right]\varphi_q(\tau)=0. \tag{3.16}$$

This is the Lamé equation for a particular value of the coefficients that make it solvable in terms of Jacobi functions [20,27].

Since the coefficients of Eq. (3.16) are periodic with period 2ω [notice that $\eta(\tau+2\omega)=-\eta(\tau)$], the mode functions can be chosen to be quasi-periodic (Floquet type) with quasi-period 2ω:

$$U_q(\tau+2\omega)=e^{iF(q)}U_q(\tau), \tag{3.17}$$

where the Floquet indices $F(q)$ are independent of τ. In the allowed zones, $F(q)$ is real and the functions $U_q(\tau)$ are bounded with a constant maximum amplitude. In the forbidden zones $F(q)$ has a non-zero imaginary part and the amplitude of the solutions either grows or decreases exponentially. The mode functions $\varphi_q(\tau)$ obey the boundary conditions, Eq. (3.2), and they are not Floquet solutions. However, they can be expressed as linear combinations of Floquet solutions [20,27] as follows:

$$\varphi_q(\tau)=\frac{1}{2\sqrt{\Omega_q}}\left[\left(1-\frac{2i\Omega_q}{\mathcal{W}_q}\right)U_q(-\tau)+\left(1+\frac{2i\Omega_q}{\mathcal{W}_q}\right)U_q(\tau)\right], \tag{3.18}$$

where $U_q(0)=1$ and

$$\mathcal{W}_q=-2q\sqrt{\frac{\frac{\eta_0^2}{2}+1+q^2}{\frac{\eta_0^2}{2}-q^2}}. \tag{3.19}$$

We find *two* allowed bands and *two* forbidden bands [20,27] for Eq. (3.16). In the physical region $q^2>0$ the allowed band corresponds to

$$\frac{\eta_0^2}{2}\leqslant q^2\leqslant +\infty \tag{3.20}$$

and the forbidden band to

$$0\leqslant q^2\leqslant \frac{\eta_0^2}{2}. \tag{3.21}$$

The modes in the forbidden band, $0<q<\eta_0/\sqrt{2}$, grow exponentially with time (parametric resonance) while those in the allowed band, $\eta_0/\sqrt{2}<q<\infty$, oscillate in time with constant amplitude. Analytic expressions for all modes were given in [20,27]. The modes from the forbidden band $0<q<\eta_0/\sqrt{2}$ dominate $\Sigma(\tau)$. For $0<\tau<\tau_1$, $\Sigma(\tau)$ oscillates with an exponentially growing amplitude. This amplitude (envelope) $\Sigma_{env}(\tau)$ can be represented to a very good approximation by the formula [20,27]

$$\Sigma_{env}(\tau)=\frac{1}{N\sqrt{\tau}}e^{B\tau}, \tag{3.22}$$

where B and N are functions of η_0 given by

$$B(\eta_0)=8\sqrt{1+\eta_0^2}\hat{q}(1-4\hat{q})+O(\hat{q}^3),$$

$$N(\eta_0)=\frac{4}{\sqrt{\pi}}\sqrt{\hat{q}}\frac{(4+3\eta_0^2)\sqrt{4+5\eta_0^2}}{\eta_0^3(1+\eta_0^2)^{3/4}}[1+O(\hat{q})], \tag{3.23}$$

and the elliptic nome $\hat{q}$ can be written as a function of η_0 as

$$\hat{q}(\eta_0)=\frac{1}{2}\frac{(1+\eta_0^2)^{1/4}-(1+\eta_0^2/2)^{1/4}}{(1+\eta_0^2)^{1/4}+(1+\eta_0^2/2)^{1/4}}, \tag{3.24}$$

with an error smaller than $\sim 10^{-7}$.

Using this estimate for the quantum fluctuations $\Sigma(\tau)$, we can now estimate the value of the non-linear time scale τ_1 at which the back reaction becomes comparable to the classical terms in the differential equations. Such a time is defined by $g\Sigma(\tau_1)\sim(1+\eta_0^2/2)$. From the results presented above, we find

$$\tau_1\approx\frac{1}{B(\eta_0)}\log\left[\frac{N(\eta_0)(1+\eta_0^2/2)}{g\sqrt{B(\eta_0)}}\right]. \tag{3.25}$$

The time interval from $\tau=0$ to $\tau\sim\tau_1$ is when most of the particle production takes place. After $\tau\sim\tau_1$ the quantum fluctuation become large enough to begin shutting off the growth of the modes and particle production slows down dramatically. This dynamical time scale separates two distinct types of dynamics; for $\tau<\tau_1$ the evolution of the quantum modes $\varphi_q(\tau)$ is essentially linear, the back-reaction effects are small and particle production proceeds via parametric amplification. Recall that the zero mode $\eta(\tau)$ obeys the non-linear evolution equation (3.14). For $\tau>\tau_1$ the quantum back-reaction effects are as important as the tree level term $\eta(\tau)^2$ and the dynamics is fully non-linear.

We plot, in Fig. 1, τ_1 as a function of the initial amplitude η_0 for different values of the coupling g.

The growth of the unstable modes in the forbidden band shows that particles are created copiously ($\sim 1/g$ for $\tau\sim\tau_1$). Initially ($\tau=0$), all the energy is in the classical zero mode (expectation value). Part of this energy is rapidly transformed into particles through parametric resonance during the interval $0<\tau<\tau_1$. At the same time, the amplitude of the

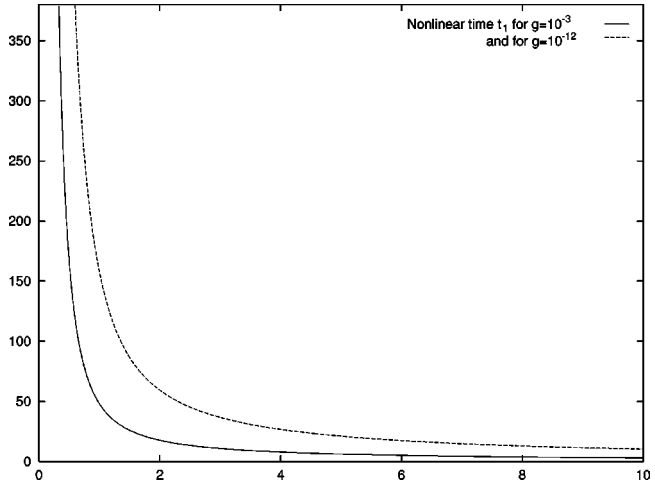

FIG. 1. The nonlinear time for the unbroken symmetry case as a function of η_0 according to Eq. (3.25) for $g=10^{-3}$ and $g=10^{-12}$.

expectation value decreases as is clearly displayed in Fig. 2. We plot in Fig. 3 the adiabatic number of particles [as defined by Eq. (3.13)] as a function of time.

The momentum distribution of the produced particles follows the Floquet index and is peaked at $q\approx\frac{1}{2}\eta_0(1-\hat{q})$ [20,27]; this is shown in Fig. 4.

IV. ASYMPTOTIC NONLINEAR EVOLUTION

A. Numerical analysis

In the previous section we have summarized the dynamical evolution in the *linear* regime in which the back-reaction effects can be neglected and estimated the *first* new, nonperturbative dynamical time scale τ_1 as that beyond which the dynamics is fully non-linear.

In this section we present the time evolution *after* the nonlinear time τ_1, that is, when the back reaction $g\Sigma(\tau)$ is important and the full solutions to the non-linear equations (3.1)–(3.3) are needed. We have implemented a refined numerical treatment for a wide range of initial amplitudes and couplings. The numerical method uses a fourth order Runge-Kutta algorithm and 16-point Gauss integrations for the integrals over q and is appended with a fast Fourier transform (FFT) analysis to determine the frequency spectrum of the oscillatory component. The precision of our results is better than 1 part in 10^5.

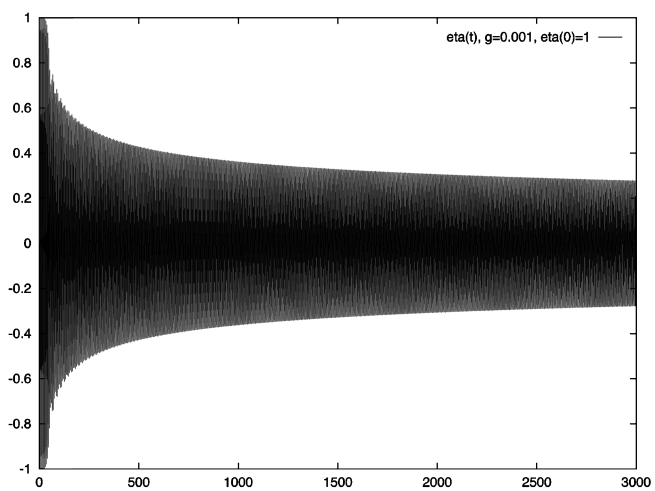

FIG. 2. The zero mode $\eta(\tau)$ vs τ for the unbroken symmetry case with $\eta_0=1$, $g=10^{-3}$.

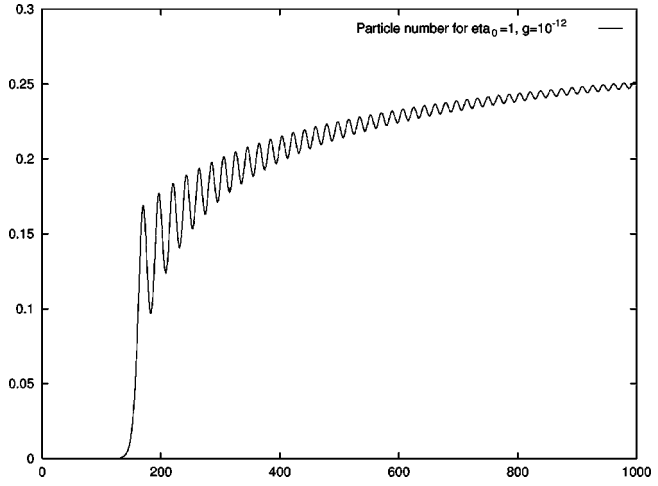

FIG. 3. The total number of produced particles as a function of time for $\eta_0=1$, $g=10^{-12}$. After the exponential increase around $\tau=\tau_1=163.7\ldots$, $\mathcal{N}^{ad}(\tau)$ keeps growing. For times $\tau>200$, Eq. (4.30) gives a very good approximation to the numerical results (after averaging over oscillations).

To begin with, we observe that $g\Sigma(\tau)$ and $\eta^2(\tau)$ oscillate with the same frequency and *opposite* phase. Thus, a remarkably cancellation takes place between these two terms in the effective mass squared. This phase opposition is analogous to Landau damping [14]. One sees such a cancellation comparing Fig. 2 for $\eta(\tau)$, Fig. 5 for $g\Sigma(\tau)$ and Fig. 6 for $\mathcal{M}^2(\tau)$.

Moreover, we see that $\mathcal{M}^2(\tau)$ tends to a constant value for $\tau\to\infty$. We find numerically that this value turns out to be

$$\mathcal{M}^2_\infty=1+\frac{\eta_0^2}{2} \tag{4.1}$$

for the values of g and η_0 considered in Figs. 1–12 (up to corrections of order g that are beyond our numerical preci-

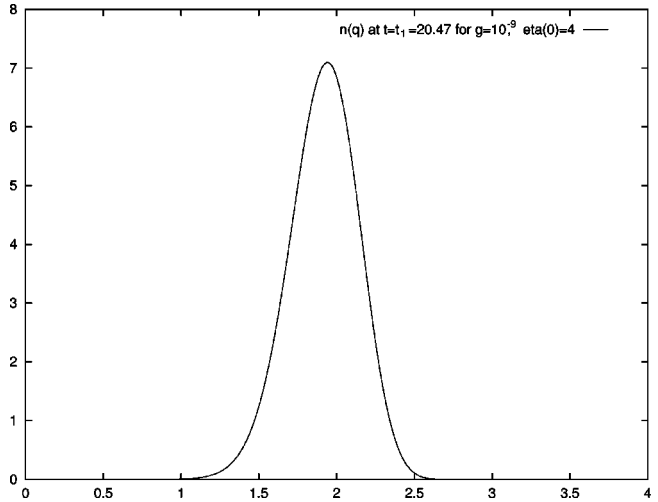

FIG. 4. Momentum distribution of the produced particles $n(q)\equiv q^2N_q^{ad}(\tau)$ at the nonlinear time $\tau=\tau_1$ for $\eta_0=4$, $g=10^{-9}$.

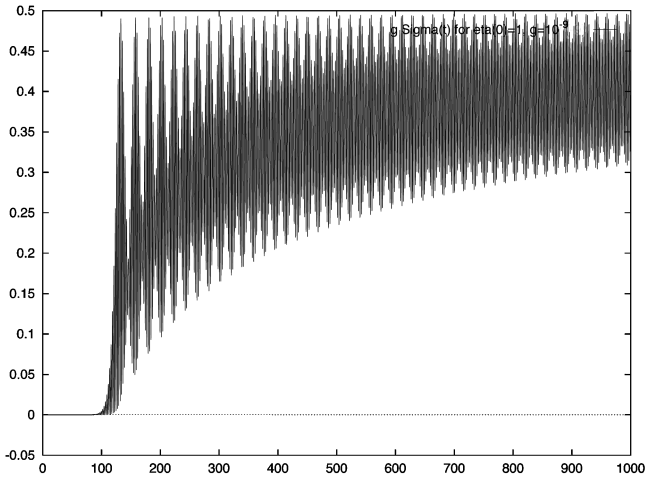

FIG. 5. The quantum fluctuations $g\Sigma(\tau)$ as a function of time for $\eta_0=1$, $g=10^{-9}$.

sion). It must be noticed that $\mathcal{M}_\infty^2$ coincides with the lower border of the allowed band (3.20).

Furthermore $\mathcal{M}^2(\tau)$ approaches its asymptotic limit (4.1), oscillating with decreasing amplitude. More precisely, using a detailed numerical analysis of the asymptotic behavior and fast Fourier transforms we find, from our numerical results for $\tau>\tau_1$ [see Figs. 6(a) and 6(b)],

$$\mathcal{M}^2(\tau)=\mathcal{M}_\infty^2+\frac{p_1(\tau)}{\tau}+\mathcal{O}\left(\frac{1}{\tau^2}\right) \tag{4.2}$$

with

$$p_1(\tau)=K_1\cos[2\mathcal{M}_\infty\tau+2a_2\log(\tau/\tau_1)+\gamma_1]+K_2\cos[2\mathcal{M}_0\tau +2b_2\log(\tau/\tau_1)+\gamma_2], \tag{4.3}$$

where K_1, K_2, γ_1 and γ_2 are constants and an excellent numerical fit for the coefficients a_2 and b_2 is given by

$$a_2\approx 0.16\ \ln\frac{1}{g}+0.6$$

$$b_2\approx 0.6-0.16\ \ln\frac{1}{g} \tag{4.4}$$

within a wide range of (weak) couplings and initial values of $\eta(0)$. We also find that the coefficients K_1, K_2 vary linearly with $\ln(1/g)$ a result that will be obtained self-consistently below.

Since the effective mass tends asymptotically to the constant value $\mathcal{M}_\infty$, the expectation value $\eta(\tau)$ oscillates with frequency $\mathcal{M}_\infty$ and the q-modes $\varphi_q(\tau)$ with frequency

$$\omega(q)\equiv\sqrt{q^2+\mathcal{M}_\infty^2}. \tag{4.5}$$

[Notice that $\omega(q)=\omega_q(\tau=+\infty)$.] These oscillation frequencies are confirmed by the numerical analysis of the evolution of the expectation value and the q-modes. Figures 7(a)–7(c) display the momentum distribution of the created particles at different times. One of the noteworthy features is that whereas up to time $\tau\approx\tau_1$ the distribution only has one peak at the value of maximum Floquet exponent, for larger times

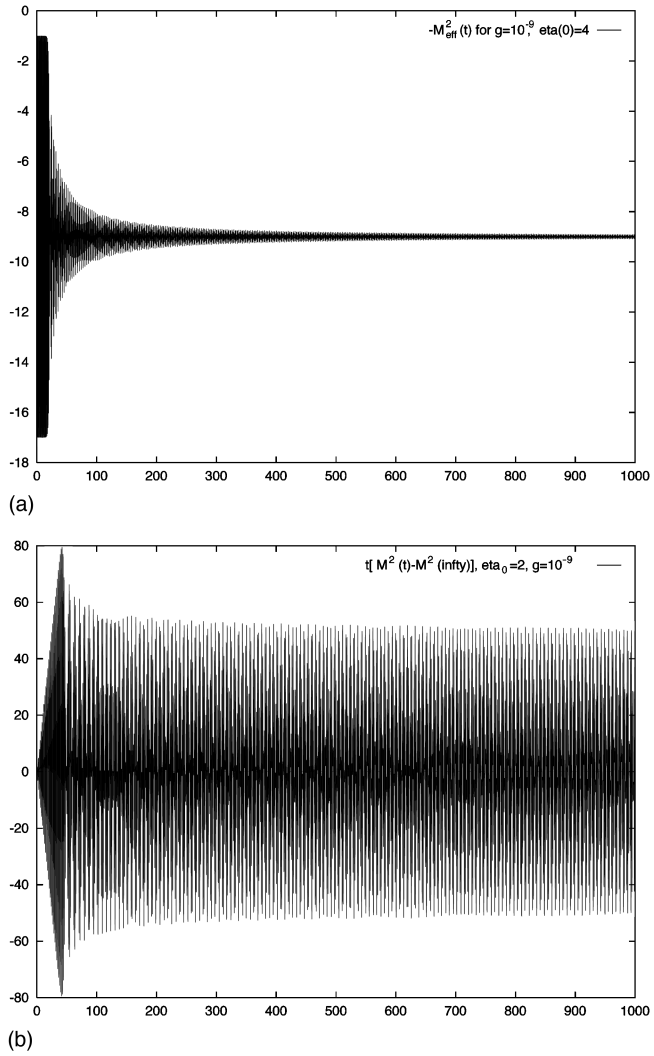

FIG. 6. (a) The effective mass squared as a function of time for $\eta_0=4$, $g=10^{-9}$. Notice the asymptotic value $\approx 1+\eta_0^2/2=9$. (b) The effective mass squared minus its value at $\tau=\infty$ times τ as a function of time for $\eta_0=2$, $g=10^{-9}$. This function oscillates in time with constant amplitude K_1+K_2 and frequencies $2\mathcal{M}_\infty=2\sqrt{1+\eta_0^2/2}$ and $2\mathcal{M}_0=2\sqrt{1+\eta_0^2}$ [see Eq. (4.3)].

the back-reaction effects introduce new structure and oscillations, keeping the *borders* of the band fixed throughout the evolution in the non-linear regime.

The numerical results displayed in Figs. 7(a)–7(c) show that the position of the main peak $q_0(\tau)$ decreases with time. We performed a numerical fit for the time dependence of the peak position and found its behavior to be well described by the estimate

$$q_0^2(\tau)\approx\frac{K_1}{\tau}, \tag{4.6}$$

with the constant K_1 introduced in Eq. (4.3) above. We will provide an analytic, self-consistent description of this behavior below.

q-modes above and below q_0 behave quite differently. Modes with $q>q_0(\tau)$ oscillate in time with constant amplitude. Modes with $q<q_0(\tau)$ also oscillate but with increasing amplitude.

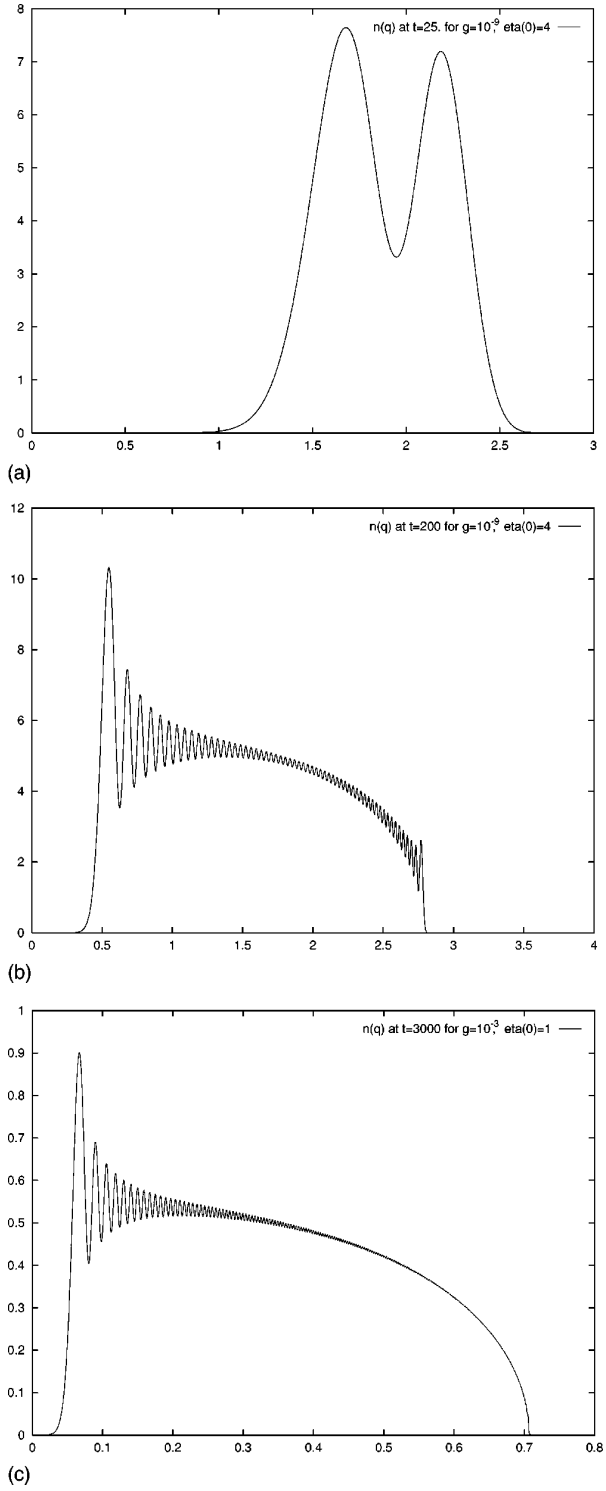

FIG. 7. (a) Momentum distribution of the produced particles at $\tau=25$ for $\eta_0=4$, $g=10^{-9}$. Notice that the single peak present for times $\tau<\tau_1$ splits into two due to the nonlinear resonances. Many more peaks appear for subsequent times as shown in (b). (b) Momentum distribution of the produced particles at $\tau=200$ for $\eta_0=4$, $g=10^{-9}$. Notice the main peak at $q=0.549$ associated with the main non-linear resonance ($q=0$) and the secondary peak at $q=2.77$ associated with the non-linear resonance at $q=\eta_0/\sqrt{2}$. The positions of both peaks are correctly estimated by Eqs. (4.6) and (4.43), respectively. (c) Momentum distribution of the produced particles at $\tau=3000$ for $\eta_0=1$, $g=10^{-3}$. Notice the main peak at $q=0.067$, in good agreement with the estimate given by Eq. (4.6).

Equation (4.6) shows that the peak position in q decreases monotonically as $\sim 1/\sqrt{\tau}$. As time evolves, more and more q-modes cross the peak and become purely oscillatory. Only the amplitude of the $q\equiv 0$ mode [which is not to be confused with the expectation value $\eta(\tau)$] keeps growing. As we shall discuss in detail below, there is a band of *non-linear* unstability for $0<q<q_0(\tau)$. We also find, numerically, that a second non-linear resonance band appears just below $q=\eta_0/\sqrt{2}$ for $q_1(\tau)<q<\eta_0/\sqrt{2}$, and we find numerically that

$$q_1^2(\tau)\approx\frac{\eta_0^2}{2}-\frac{\sqrt{2}K_2}{\tau}. \tag{4.7}$$

However, the growing modes in this upper band give a much less important contribution to the physical magnitudes than the first band.

The modes in between, $q_0(\tau)<q<q_1(\tau)$, oscillate for times $\tau>\tau_1$ with stationary amplitude $M_q(\tau)$.

This crossover behavior of the modes can be expressed by introducing a q-dependent time scale beyond which the modes become oscillatory. Such scale is given by

$$\tau_I(q)=\frac{K_1}{q^2} \tag{4.8}$$

for the lower nonlinear band and

$$\tau_{II}(q)=\frac{K_2}{\frac{\eta_0^2}{2}-q^2} \tag{4.9}$$

for the upper nonlinear band.

Both $\varphi_{q=0}(\tau)$ and $\eta(\tau)$ obey Eq. (3.1) and are linearly independent solutions, their difference arising from the initial conditions. $\varphi_{q=0}(\tau)$ has a growing amplitude while the amplitude of $\eta(\tau)$ decreases with time. Since these are linearly independent solutions of the same equation, their Wronskian is a non-vanishing constant. Therefore if one solution grows, the other independent solution must decrease in order to respect the Wronskian condition (3.6). Since the total energy is conserved, $\eta(\tau)$ must necessarily be a decreasing solution.

The fact that the zero-mode amplitude $\eta(\tau)$ vanishes for $\tau=\infty$ implies that *all* the available energy transforms into particles for $\tau=\infty$. This conclusion which will be further clarified in what follows is a consequence of the non-linear dynamics. It is the more remarkable because the particles produced are *massive* and therefore there is a threshold to *perturbative* particle production. It will be seen in detail below that the particle production in this regime is a truly non-perturbative phenomenon associated with non-linear resonances.

For $\tau>\tau_1,\tau_I(q),\tau_{II}(q)$ the effective mass squared tends to a constant [see Eq. (4.1)]; therefore, the asymptotic behavior of $\varphi_q(\tau)$ is given by

$$\varphi_q(\tau)\overset{\tau\to\infty}{=}A_q e^{i\omega(q)\tau}+B_q e^{-i\omega(q)\tau}+\mathcal{O}\left(\frac{1}{\tau}\right) \tag{4.10}$$

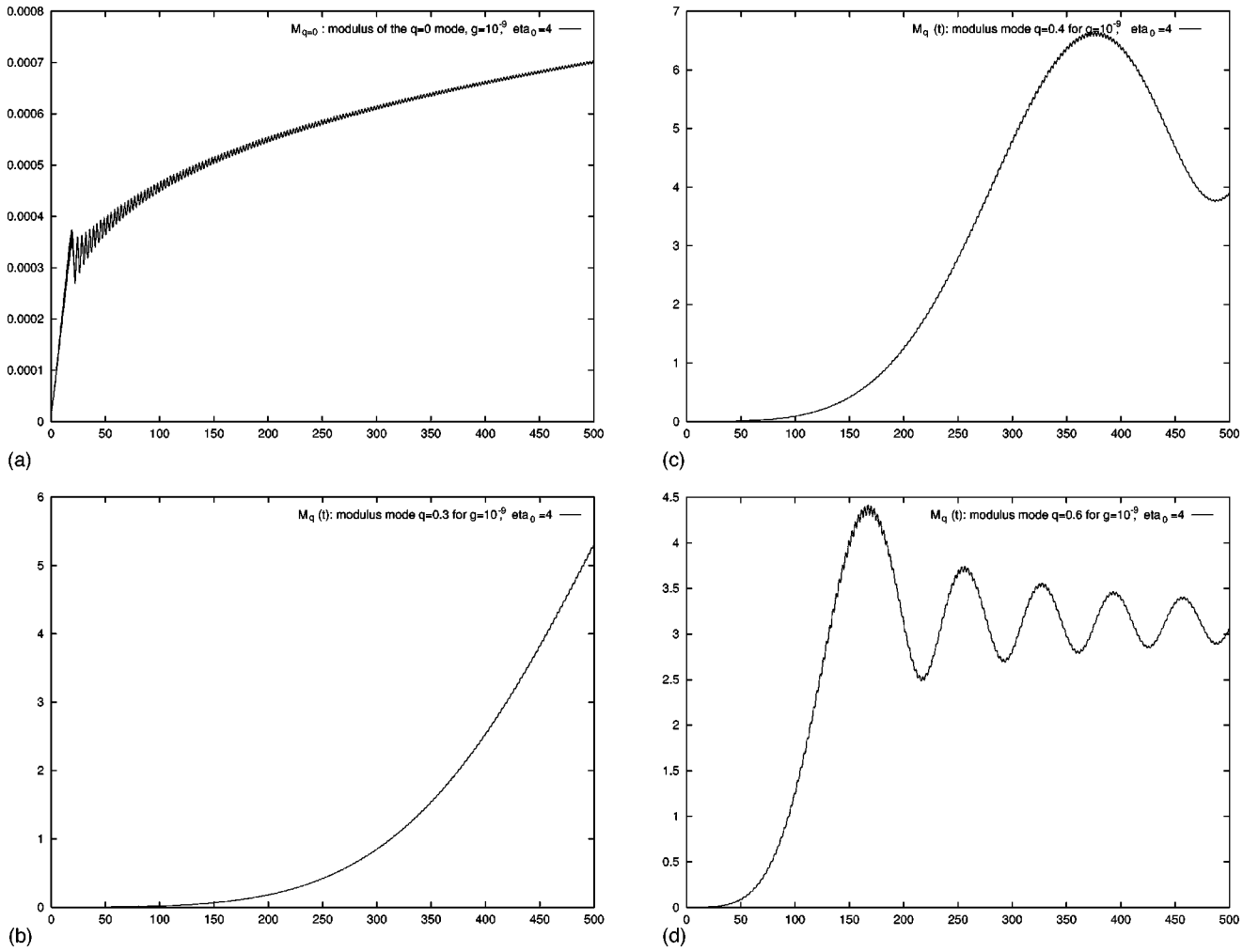

FIG. 8. (a) The amplitude $M_q(\tau)$ of the mode function $\varphi_{q=0}(\tau)$ as a function of time for $\eta_0=4$, $g=10^{-9}$. It grows as a power according to Eq. (4.22). (b) The amplitude $M_q(\tau)$ of the mode function $\varphi_{q=0.3}(\tau)$ as a function of time for $\eta_0=4$, $g=10^{-9}$. This amplitude grows faster for $\tau>\tau_1$ than the $q=0$ amplitude but much slower than the exponential growth in the forbidden band $0<q<\eta_0/\sqrt{2}$ for $\tau<\tau_1$. (c) The amplitude $M_q(\tau)$ of the mode function $\varphi_{q=0.4}(\tau)$ as a function of time for $\eta_0=4$, $g=10^{-9}$. This mode grows until $\tau\sim K_1/q^2\sim 350$. At such time this mode crosses out of the nonlinear resonance band. (d) The amplitude $M_q(\tau)$ of the mode function $\varphi_{q=0.6}(\tau)$ as a function of time for $\eta_0=4$, $g=10^{-9}$. This mode grows until $\tau\sim K_1/q^2\sim 150$. At such time the mode crosses out of the nonlinear resonance band.

with $\omega(q)$ given by Eq. (4.5). It is then convenient to define the following functions:

$$A_q(\tau)\equiv\frac{1}{2}e^{-i\omega(q)\tau}\left[\varphi_q(\tau)-\frac{i}{\omega(q)}\dot{\varphi}_q(\tau)\right],$$

$$B_q(\tau)\equiv\frac{1}{2}e^{+i\omega(q)\tau}\left[\varphi_q(\tau)+\frac{i}{\omega(q)}\dot{\varphi}_q(\tau)\right], \qquad (4.11)$$

which for $\tau>\tau_1$ are slowly varying functions of τ, with the asymptotic limits

$$\lim_{\tau\to\infty}A_q(\tau)=A_q, \quad \lim_{\tau\to\infty}B_q(\tau)=B_q. \qquad (4.12)$$

We can thus express the mode functions $\varphi_q(\tau)$ in terms of $A_q(\tau)$ and $B_q(\tau)$ as follows:

$$\varphi_q(\tau)=A_q(\tau)e^{i\omega(q)\tau}+B_q(\tau)e^{-i\omega(q)\tau}. \qquad (4.13)$$

We obtain from Eq. (4.11), for the square modulus of the modes,

$$|\varphi_q(\tau)|^2=|A_q(\tau)|^2+|B_q(\tau)|^2+2|A_q(\tau)B_q(\tau)|\cos[2\omega(q)\tau+\phi_q(\tau)] \qquad (4.14)$$

where we have set

$$A_q(\tau)B_q(\tau)^*=|A_q(\tau)B_q(\tau)|e^{i\phi_q(\tau)}. \qquad (4.15)$$

The Wronskian relation (3.6) implies that the functions $A_q(\tau)$ and $B_q(\tau)$ are related asymptotically through

$$|B_q(\tau)|^2-|A_q(\tau)|^2=\frac{1}{\omega(q)} \qquad (4.16)$$

plus terms that vanish asymptotically. The virtue of introducing the amplitudes $A_q(\tau)$, $B_q(\tau)$ is that their variation in τ is slow, because the rapid variation of the mode functions is accounted for by the phase.

Figures 8–11 show the (scaled) modulus

$$M_q(\tau)\equiv\sqrt{g}\sqrt{|A_q(\tau)|^2+|B_q(\tau)|^2} \qquad (4.17)$$

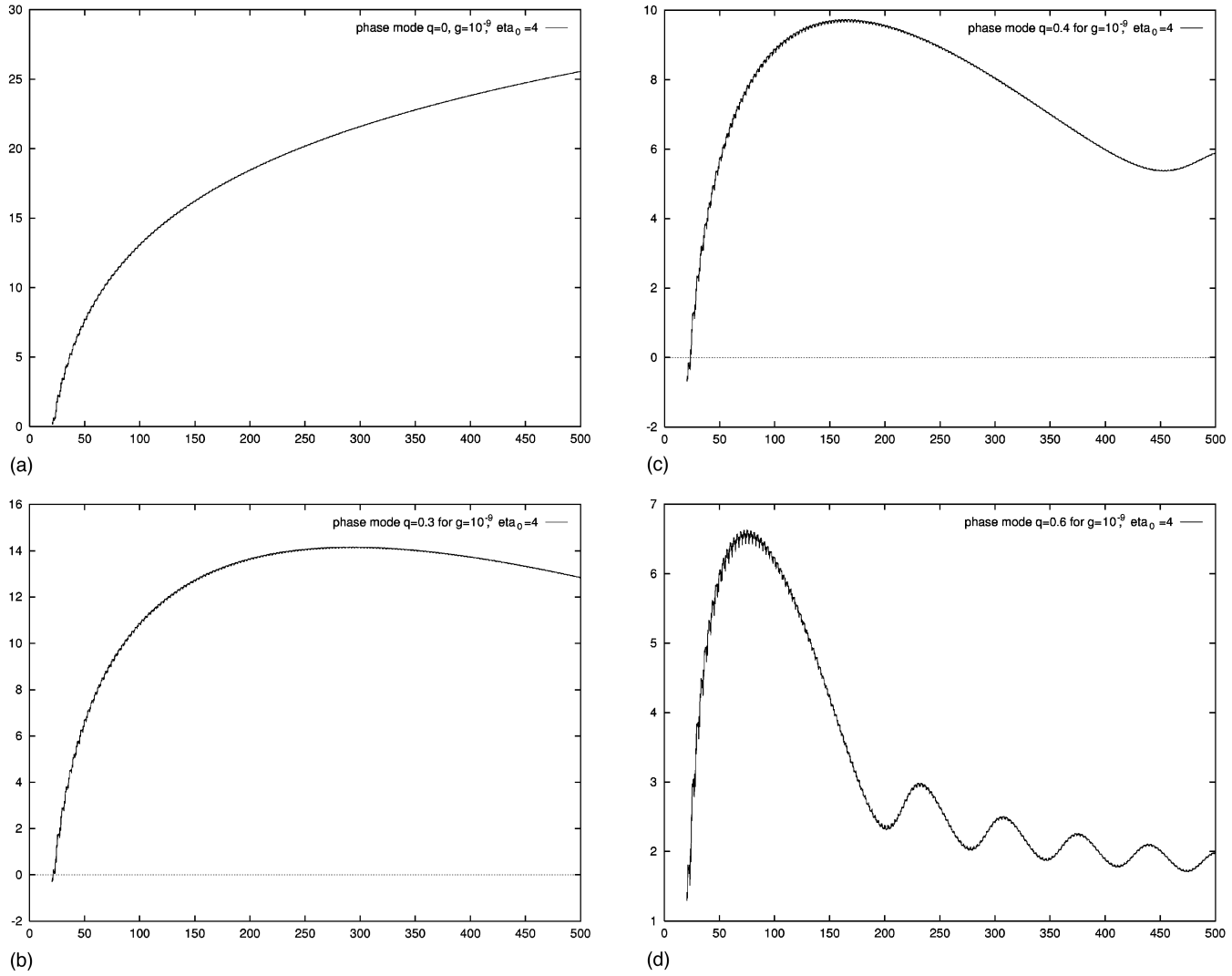

FIG. 9. (a) The phase $\phi_q(\tau)$ of the mode function $\varphi_{q=0}(\tau)$ as a function of time for $\eta_0=4$, $g=10^{-9}$. This function follows Eq. (4.22) with a very good approximation. (b) The phase $\phi_q(\tau)$ of the mode function $\varphi_{q=0.3}(\tau)$ as a function of time for $\eta_0=4$, $g=10^{-9}$. (c) The phase $\phi_q(\tau)$ of the mode function $\varphi_{q=0.4}(\tau)$ as a function of time for $\eta_0=4$, $g=10^{-9}$. (d) The phase $\phi_q(\tau)$ of the mode function $\varphi_{q=0.6}(\tau)$ as a function of time for $\eta_0=4$, $g=10^{-9}$. This phase becomes an oscillatory function as the same time as the modulus $M_q(\tau)$ [see Fig. 8(d)] stops growing.

and $\phi_q(\tau)$ for some relevant cases. As shown in these figures $M_q(\tau)$ and $\phi_q(\tau)$ do not exhibit rapid oscillations with period $2\pi/\omega(q)$ and $2\pi/\mathcal{M}_\infty$ which are present in $\varphi_q(\tau)$ and $\eta(\tau)$, respectively. That is, as anticipated above, $M_q(\tau)$ and $\phi_q(\tau)$ vary *slowly* with τ.

For small coupling g, $|\varphi_q(\tau)|^2$,$|B_q(\tau)|^2$ and $|A_q(\tau)|^2$ are of order $1/g$ for q in the forbidden band and times later than τ_1 [20,27]. Therefore, $M_q(\tau)$ becomes of order 1 after the non-linear time scale for modes inside the band, and is perturbatively small for modes outside the band. Moreover, Eq. (4.16) implies that $|B_q(\tau)|^2=|A_q(\tau)|^2[1+O(g)]$ and for modes inside the band we can approximate Eq. (4.14) as follows:

$$g|\varphi_q(\tau)|^2=M_q(\tau)^2\{1+\cos[2\omega(q)\tau+\phi_q(\tau)]\}[1+O(g)], \tag{4.18}$$

for $0<q<\eta_0/\sqrt{2}$. This expression is very illuminating because it displays a separation between the short time scales in the argument of the cosine and the long time scales in the modulus $M_q(\tau)$ and phase $\phi_q(\tau)$.

We now introduce slowly varying coefficients for the order parameter $\eta(\tau)$. Let us define

$$D(\tau)\equiv\sqrt{\eta(\tau)^2+\dot{\eta}(\tau)^2/\mathcal{M}_\infty^2} \tag{4.19}$$

$$\phi(\tau)\equiv-\mathcal{M}_\infty\tau-\arctan\left[\frac{\dot{\eta}(\tau)}{\eta(\tau)}\right]. \tag{4.20}$$

Using the result that asymptotically the effective time dependent mass reaches the asymptotic limit $\mathcal{M}_\infty$ and the fact that $\eta(\tau)$ is a real function we write

$$\eta(\tau)=D(\tau)\ \cos[\mathcal{M}_\infty\tau+\phi(\tau)]\left[1+\mathcal{O}\left(\frac{1}{\tau}\right)\right]. \tag{4.21}$$

We plot, in Figs. 12, $D(\tau)$ and $\phi(\tau)$ as functions of τ.

We begin our numerical analysis by considering the $q=0$ mode function. After an exhaustive analysis we have

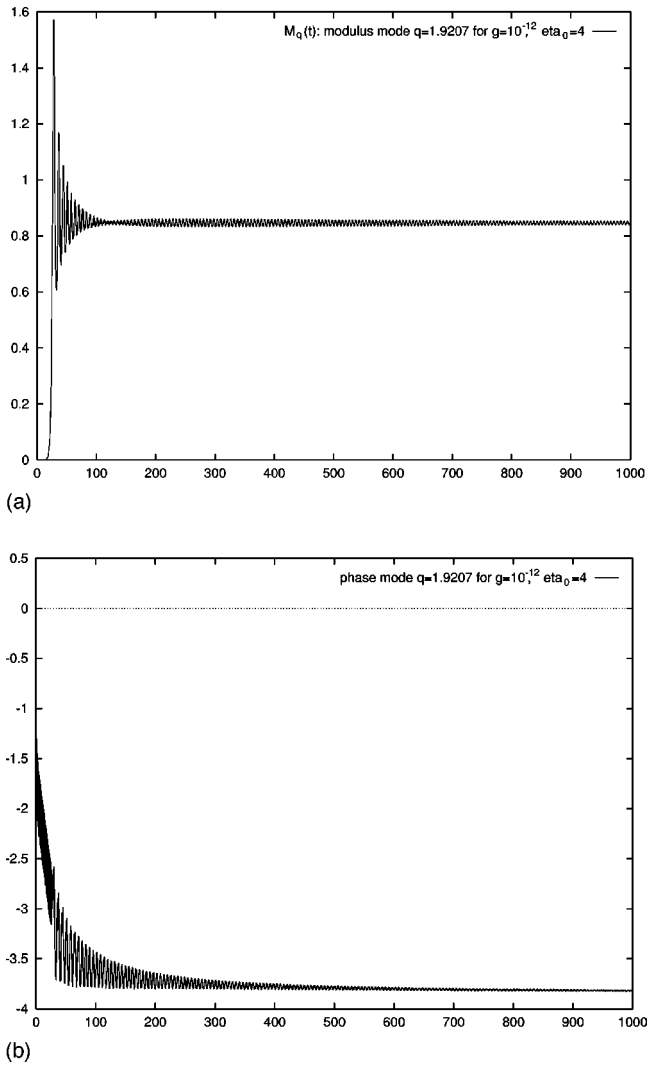

FIG. 10. (a) The modulus $M_q(\tau)$ of the mode function $\varphi_{q=1.9207}(\tau)$ as a function of time for $\eta_0=4$, $g=10^{-12}$. For times later than $\tau_1=26.85\ldots$, this mode oscillates with stationary amplitude. It lies outside both nonlinear resonance bands. (b) The phase $\phi_q(\tau)$ of the mode function $\varphi_{q=1.9207}(\tau)$ as a function of time for $\eta_0=4$, $g=10^{-12}$.

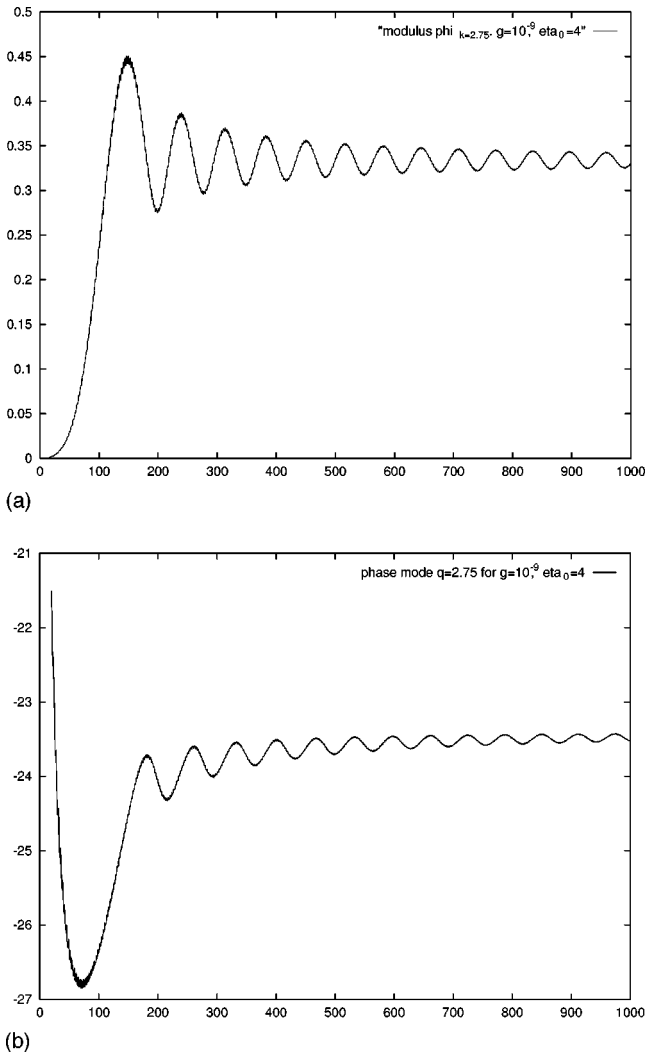

FIG. 11. (a) The modulus $M_q(\tau)$ of the mode function $\varphi_{q=2.75}(\tau)$ as a function of time for $\eta_0=4$, $g=10^{-9}$. This function grows until $q=2.75$ gets out of the second nonlinear resonance band. The estimate (4.43) ($\tau\sim 140$) is in very good agreement with the numerical results plotted here. (b) The phase $\phi_q(\tau)$ of the mode function $\varphi_{q=2.75}(\tau)$ as a function of time for $\eta_0=4$, $g=10^{-9}$. This phase changes its behavior (around $\tau\sim 140$) when the modulus $M_{q=2.75}(\tau)$ ceases to grow (a).

found that $A_{q=0}(\tau)$ and $B_{q=0}(\tau)$ exhibit power behavior for $\tau>\tau_1$ (see Figs. 8–10). To our numerical precision these power laws can be fit by the following form:

$$A_{q=0}(\tau)\approx\tau^{ia_2}[C_1\tau^{a_1}+C_2\tau^{-a_1}],$$
$$B_{q=0}(\tau)\approx\tau^{-ia_2}[C_1'\tau^{a_1}+C_2'\tau^{-a_1}], \tag{4.22}$$

where the numerical results yield, for the *anomalous dynamical exponents*,

$$a_1\approx 0.27 \tag{4.23}$$

while a_2 is the *same* as in Eqs. (4.3), (4.4).

The behavior (4.22) appears also in the evolution of the expectation value $\eta(\tau)$ but with the growing power of τ absent ($C_1=C_1'\equiv 0$) resulting in the order parameter decreasing with time, exhibiting a logarithmic phase:

$$\eta(\tau)=D_0\left(\frac{\tau}{\tau_1}\right)^{-a_1}\cos[\mathcal{M}_\infty\tau+a_2\log(\tau/\tau_1)+f_0]\left[1+\mathcal{O}\left(\frac{1}{\tau}\right)\right] \tag{4.24}$$

where f_0 is a small constant. Therefore, comparing with Eq. (4.21) we find the remarkable result that the *amplitude* of the expectation value relaxes with a dynamical power law exponent,

$$D(\tau)=D_0\left(\frac{\tau}{\tau_1}\right)^{-a_1}\left[1+\mathcal{O}\left(\frac{1}{\tau}\right)\right], \tag{4.25}$$

and a logarithmically varying phase

$$\phi(\tau)=a_2\log\left(\frac{\tau}{\tau_1}\right)+f_0+\mathcal{O}\left(\frac{1}{\tau}\right). \tag{4.26}$$

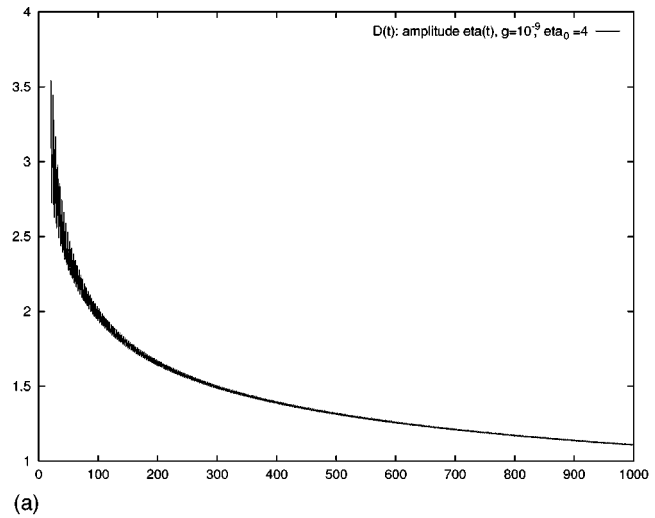

FIG. 12. (a) The amplitude $D(\tau)$ of the zero mode $\eta(\tau)$ as a function of time for $\eta_0=4$, $g=10^{-9}$. This function exhibits a power like decrease according to Eq. (4.25). (b) The phase $\phi(\tau)$ of the zero mode $\eta(\tau)$ as a function of time for $\eta_0=4$, $g=10^{-9}$. This function exhibits a logarithmic behavior according to Eq. (4.26).

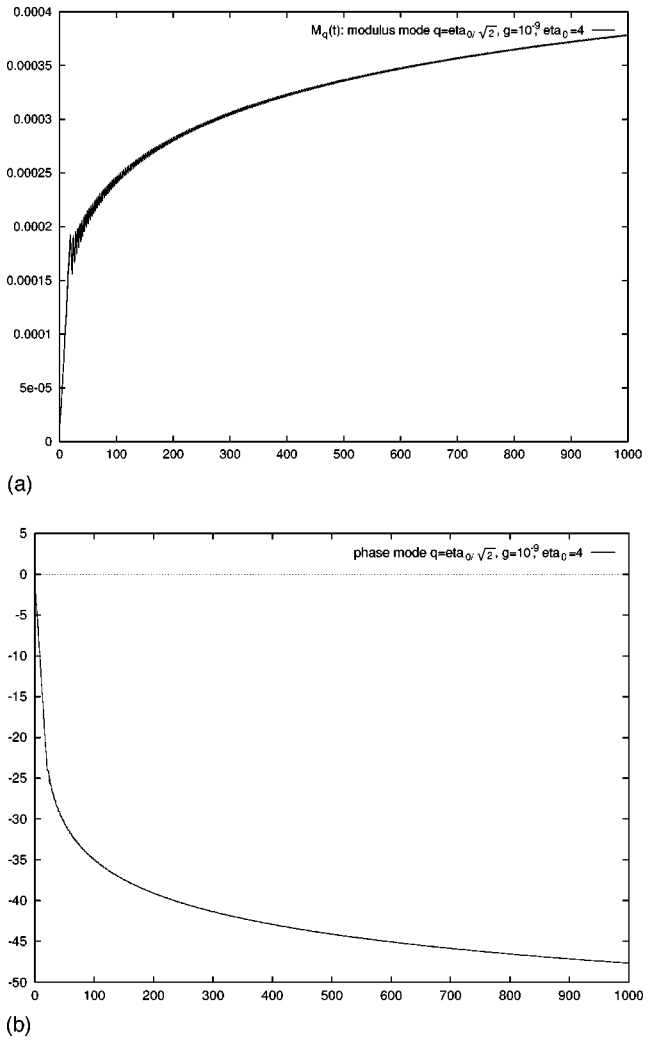

FIG. 13. (a) The amplitude $M_q(\tau)$ of the mode function $\varphi_{q=\eta_0/\sqrt{2}}(\tau)$ as a function of time for $\eta_0=4$, $g=10^{-9}$. (This corresponds to the upper border of the forbidden band.) This function exhibits a power-like increase according to Eq. (4.27). (b) The phase $\phi_q(\tau)$ of the mode function $\varphi_{q=\eta_0/\sqrt{2}}(\tau)$ as a function of time for $\eta_0=4$, $g=10^{-9}$. (This corresponds to the upper border of the forbidden band.) This phase exhibits a logarithmic behavior according to Eq. (4.27).

The time τ_1 appears here since it is the natural time scale for the non-linear phenomena.

The $q\neq 0$ modes also grow with time with a power-like behavior for $0<q<q_0(\tau)$ but with a larger power than the $q=0$ mode (see Figs. 8–10). Such growth is definitely milder than the exponential increase of the modes inside the forbidden band in parametric resonance. Our interpretation of this phenomenon is that $0<q<q_0(\tau)$ is a *non-linear* resonant band. It is not a resonance in a linear differential equation (as it is a parametric resonance), but a *new* nonlinear effect which is a consequence of the back reaction of the quantum fluctuations through $g\Sigma(\tau)$.

A second non-linear resonance band appears just below $q=\eta_0/\sqrt{2}$ for $q_1(\tau)<q<\eta_0/\sqrt{2}$. However, we find numerically that the contribution from this upper band to physical quantities such as particle production is much smaller than the first band. The modes in between, $q_0(\tau)<q<q_1(\tau)$, oscillate for times $\tau>\tau_1$ with stationary amplitude $M_q(\tau)$.

The nonlinear resonant bands become narrower as a function of time; i.e., $q_0(\tau)$ and $\eta_0/\sqrt{2}-q_1(\tau)$ decrease with time [$q_1(\tau)$ increases].

The growth of the amplitudes $M_q(\tau)$ in the nonlinear resonant bands for a fixed q stops when q crosses the borders $q_0(\tau)$ or $q_1(\tau)$. After that time, such q-modes oscillate with constant amplitude; this behavior is displayed in Fig. 8(d). There is a crossover for $q\sim q_0(\tau)$ and for $q\sim q_1(\tau)$ from monotonic growth to oscillatory behavior.

The phase $\phi_q(\tau)$ exhibits an analogous behavior [see Fig. 9(d)].

The particle distribution exhibits marked peaks at $q\approx q_0(\tau)$ and at $q\approx q_1(\tau)$, which are clearly displayed in Fig. 7. Notice that the peak near $q\approx q_1(\tau)$ has a much smaller amplitude.

The mode exactly at $q=\eta_0/\sqrt{2}$ has an analogous behavior to the $q=0$ mode (compare Fig. 13 with Fig. 8). We find to our numerical accuracy that the amplitudes behave as

$$A_{q=\eta_0/\sqrt{2}}(\tau)\approx\tau^{ib_2}[E_1\tau^{b_1}+E_2\tau^{-b_1}],$$

$$B_{q=\eta_0/\sqrt{2}}(\tau)\approx\tau^{-ib_2}[E_1'\tau^{b_1}+E_2'\tau^{-b_1}]. \tag{4.27}$$

The numerical calculations yield, for the dynamical exponents,

$$b_1\approx 0.19 \tag{4.28}$$

and b_2 is the *same* exponent as in Eqs. (4.3), (4.4).

The growth of the q-modes in both nonlinear resonant bands leads to particle production. We see from Fig. 3 that the number of particles continues to grow after the nonlinear time $\tau=\tau_1$. Although this growth is *much slower* than before $\tau=\tau_1$, the total number of particles produced *after* the time τ_1 is substantial and turns to be of the same order of magnitude than those produced before τ_1.

The adiabatic number of produced particles, $N_q^{ad}(\tau)$, can be expressed for late times in terms of the mode amplitudes $M_q(\tau)$ as follows:

$$N_q^{ad}(\tau)=\frac{1}{2g}\omega(q)M_q(\infty)^2+\mathcal{O}\left(\frac{1}{\tau}\right)+\mathcal{O}(g) \tag{4.29}$$

where we used Eqs. (3.12), (4.10) and (4.17). Notice that asymptotically the adiabatic particle number depends solely on the long time scale as the terms containing the fast oscillating function $\cos[2\omega(q)\tau+\phi_q(\tau)]$ cancel out to order τ^0 for large τ. This is one of the important advantages of this definition of the particle number.

For $\tau\gg\tau_1$ the total number of produced particles approaches its asymptotic value $\mathcal{N}^{ad}(\infty)$ as

$$\mathcal{N}^{ad}(\tau)=\mathcal{N}^{ad}(\infty)-\frac{G}{\tau}+\mathcal{O}\left(\frac{1}{\tau^2}\right), \tag{4.30}$$

where

$$g\mathcal{N}^{ad}(\infty)=\frac{1}{4\pi^2}\int_0^{\eta_0/\sqrt{2}}q^2dq\,\omega(q)M_q(\infty)^2+\mathcal{O}(g) \tag{4.31}$$

and G is positive.

The numerical analysis shows that $g\mathcal{N}^{ad}(\infty)$ and gG depend very little on g for small $g<10^{-3}$. Both $\mathcal{N}^{ad}(\infty)$ and G grow with η_0. Precise numerical fits yield the behavior

$$g\mathcal{N}^{ad}(\infty)\sim 0.007\,\eta_0^{2.8} \tag{4.32}$$

for a wide range of couplings and η_0.

At this point we summarize the results from the numerical analysis for the unbroken symmetry case:

The effective time dependent mass reaches a finite asymptotic value $\mathcal{M}_\infty$ in the form given by Eqs. (4.2), (4.3), (4.4). This in turn means that the modes become *free* asymptotically with plane wave behavior and the non-linear self-consistent coupling between modes vanishes. The large N limit yields free modes in the infinite time limit.

For weak coupling and for $\tau>\tau_1$ there is a separation of time scales, with a short time scale corresponding to oscillations with frequencies corresponding to a mass $\approx\mathcal{M}_\infty$ and a longer time scale that depends on τ_1.

The amplitude of the expectation value relaxes with a power law with *non-universal* dynamical exponents and logarithmic phases that vary solely on the long time scale. The expectation value vanishes asymptotically, despite the fact that its energy is dissipated into massive particles for which there are perturbative thresholds for production. The relaxation mechanism is *non-linear* and clearly non-perturbative even at long times.

For $\tau>\tau_1$ there are non-linear resonant bands which form at the edges of the original band for parametric amplification. The width of these non-linear resonant bands vanishes asymptotically, resulting in all modes oscillating harmonically for asymptotically large time. For $\tau=\infty$ both unstable non-linear bands $[0<q<q_0(\tau)$ and $q_1(\tau)<q<\eta_0/\sqrt{2}]$ shrink to zero. The crossover from power-like to oscillatory behavior takes place at the q-dependent time scales given by Eqs. (4.8), (4.9).

The particle distribution $N_q^{ad}(\tau)$ has a finite and nontrivial limit for $\tau\to\infty$. In particular, a consequence of the non-linear resonant bands is that $N_q^{ad}(\infty)$ will be peaked at $q=0$. The asymptotic form of the distribution is a function of the initial conditions and the coupling g. In particular, $N_q^{ad}(\infty)$ is of order $1/g$ for $q<\eta_0/\sqrt{2}$ and it is of order 1 for $q>\eta_0/\sqrt{2}$. That is, the support of the particle distribution valid for short times $\tau<\tau_1$ survives for all times including $\tau=\infty$. Furthermore, for weak coupling the large number of particles inside this band allows us to interpret this asymptotic state as a non-perturbative semiclassical condensate in the unbroken symmetry phase that has formed dynamically through the relaxation of the initial energy.

B. Asymptotic analysis I: Perturbation theory

In the previous section we presented an exhaustive numerical study of the evolution of the mode functions and the expectation value. In this section we provide an analytic perturbative approach to explain and understand the numerical results.

In order to study analytically the asymptotic behavior for late times, it is convenient to write the equations for the expectation value and mode functions as follows:

$$\left[\frac{d^2}{d\tau^2}+q^2+\mathcal{M}_\infty^2+w(\tau)\right]\varphi_q(\tau)=0,$$

$$\left[\frac{d^2}{d\tau^2}+\mathcal{M}_\infty^2+w(\tau)\right]\eta(\tau)=0 \tag{4.33}$$

where

$$w(\tau)\equiv\mathcal{M}^2(\tau)-\mathcal{M}_\infty^2=\frac{p_1(\tau)}{\tau}+\mathcal{O}\left(\frac{1}{\tau^2}\right) \tag{4.34}$$

and $p_1(\tau)$ given by Eq. (4.3) will be treated as a small perturbation for $\tau\gg\tau_1$.

These equations can be written as integral equations using the proper Green's function. That is,

$$\varphi_q(\tau)=A_q e^{i\omega(q)\tau}+B_q e^{-i\omega(q)\tau} - \int_\tau^\infty d\tau' \frac{\sin\,\omega(q)(\tau'-\tau)}{\omega(q)} w(\tau')\varphi_q(\tau'). \tag{4.35}$$

Here we used the advanced Green's function that obeys

$$\left[\frac{d^2}{d\tau^2}+q^2+\mathcal{M}_\infty^2\right]\left\{\theta(\tau'-\tau)\frac{\sin[\,\omega(q)(\tau'-\tau)]}{\omega(q)}\right\}=\delta(\tau-\tau'). \tag{4.36}$$

Since $w(\tau)=\mathcal{O}(1/\tau)$, we can generate the asymptotic expansion for $\varphi_q(\tau)$ just by iterating Eq. (4.35). We find

$$\varphi_q(\tau)=A_q e^{i\omega(q)\tau}+B_q e^{-i\omega(q)\tau} - \int_\tau^\infty d\tau' \frac{\sin\,\omega(q)(\tau'-\tau)}{\omega(q)}\,\frac{p_1(\tau')}{\tau'}[A_q e^{i\omega(q)\tau'} + B_q e^{-i\omega(q)\tau'}]d\tau'+\mathcal{O}\left(\frac{1}{\tau^2}\right). \tag{4.37}$$

The integrals here can be performed in closed form up to terms of $\mathcal{O}(1/\tau^2)$ by using Eq. (4.3) for $p_1(\tau)$. The result is given by

$$\begin{aligned}\varphi_q(\tau)=&\left(A_q\left[1+\frac{K_1\,\sin\,\Psi_1(\tau)}{4i\mathcal{M}_\infty\omega(q)\tau}+\frac{K_2\,\sin\,\Psi_2(\tau)}{4i\mathcal{M}_0\omega(q)\tau}\right]\right.\\ &+\frac{B_q}{8\omega(q)\tau}\left\{K_1\left[\frac{e^{i(\Psi_1(\tau)-2\tau\omega(q))}}{\omega(q)-\mathcal{M}_\infty}+\frac{e^{-i(\Psi_1(\tau)+2\tau\omega(q))}}{\omega(q)+\mathcal{M}_\infty}\right]\right.\\ &\left.\left.+K_2\left[\frac{e^{i(\Psi_2(\tau)-2\tau\omega(q))}}{\omega(q)-\mathcal{M}_0}+\frac{e^{-i(\Psi_2(\tau)+2\tau\omega(q))}}{\omega(q)+\mathcal{M}_0}\right]\right\}\right)e^{i\omega(q)\tau}\\ &+\left(B_q\left[1-\frac{K_1\,\sin\,\Psi_1(\tau)}{4i\mathcal{M}_\infty\omega(q)\tau}-\frac{K_2\,\sin\,\Psi_2(\tau)}{4i\mathcal{M}_0\omega(q)\tau}\right]\right.\\ &+\frac{A_q}{8\omega(q)\tau}\left\{K_1\left[\frac{e^{-i(\Psi_1(\tau)-2\tau\omega(q))}}{\omega(q)-\mathcal{M}_\infty}+\frac{e^{i(\Psi_1(\tau)+2\tau\omega(q))}}{\omega(q)+\mathcal{M}_\infty}\right]\right.\\ &+K_2\left[\frac{e^{-i(\Psi_2(\tau)-2\tau\omega(q))}}{\omega(q)-\mathcal{M}_0}\right.\\ &\left.\left.\left.+\frac{e^{i(\Psi_2(\tau)+2\tau\omega(q))}}{\omega(q)+\mathcal{M}_0}\right]\right\}\right)e^{-i\omega(q)\tau}+\mathcal{O}\left(\frac{1}{\tau^2}\right),\end{aligned} \tag{4.38}$$

where

$$\Psi_1(\tau)\equiv 2\mathcal{M}_\infty\tau+2a_2\,\log\frac{\tau}{\tau_1}+\gamma_1$$

and

$$\Psi_2(\tau)\equiv 2\mathcal{M}_0\tau+2b_2\,\log\frac{\tau}{\tau_1}+\gamma_2.$$

These expressions display resonant denominators for $\omega(q)=\mathcal{M}_\infty$ and $\omega(q)=\mathcal{M}_0$. These resonances correspond to $q=0$ and $q=\eta_0/\sqrt{2}$, respectively. This perturbative approach is expected to be valid when the first order correction is smaller than the zeroth order correction. A necessary condition for its validity is given by

$$\frac{K_1}{\omega(q)\tau[\,\omega(q)-\mathcal{M}_\infty]}<1. \tag{4.39}$$

This implies, for q significatively smaller than $\mathcal{M}_\infty$,

$$q^2>\frac{K_1}{\tau}, \tag{4.40}$$

where we approximated

$$\omega(q)\simeq\mathcal{M}_\infty+\frac{q^2}{2\mathcal{M}_\infty}. \tag{4.41}$$

Thus in the regime where Eq. (4.40) holds the behavior of the mode functions is *oscillatory* and given by Eq. (4.38). This is in agreement with the numerical results discussed in Sec. IV A. The equality sign in Eq. (4.40) yields Eq. (4.6) for the peak position which was found numerically and therefore now interpreted as the result of a resonance condition. Such peaks can be seen also in the mode functions amplitudes displayed in Figs. 8, 11.

The resonance at $q=\eta_0/\sqrt{2}$ can be treated analogously. The necessary condition for the validity of the perturbative approach is then

$$\frac{K_2}{\omega(q)\tau[\,\omega(q)-\mathcal{M}_0]}<1.$$

Near $q=\eta_0/\sqrt{2}$ we can write

$$\omega(q)\simeq\mathcal{M}_0+\frac{\eta_0(q-\eta_0/\sqrt{2})}{\sqrt{2}\mathcal{M}_0}.$$

Therefore, the oscillatory behavior (4.38) applies for

$$\frac{\eta_0}{\sqrt{2}}-q>\frac{K_2}{\eta_0\tau}. \tag{4.42}$$

The equality sign in Eq. (4.42) yields the peak positions of the mode function amplitudes near such resonance:

$$q_1(\tau)=\frac{\eta_0}{\sqrt{2}}-\frac{K_2}{\eta_0\tau}. \tag{4.43}$$

These results are in remarkable agreement with our numerical calculations (see Figs. 8, 11).

The position of the main peak in the particle distributions precisely corresponds to the situation where q^2 is balanced by the amplitude in the ''potential'' $-p_1(\tau)/\tau$. Namely, for $q^2>K_1/\tau$, we have oscillating modes and, for $q^2<K_1/\tau$, resonant (growing) modes. The same argument applies to the secondary peak.

C. Asymptotic analysis II: Multitime scales

The perturbative analysis took us a long ways towards understanding the presence of the non-linear resonances as-

sociated with back-reaction effects and revealed the position of these resonances in complete agreement with the numerical study.

However, to describe the evolution of the modes *inside* these bands the perturbative approach is insufficient and a non-perturbative method of resumming the potential secular terms associated with the resonances must be implemented.

The main observation from the numerical analysis is that for weak coupling there are two widely separated time scales, the short time scale associated with oscillations with frequency determined by the asymptotic value of the effective mass and a long scale associated with the non-linear time τ_1. This suggests to implement a multitime scale analysis [28] which resums the secular terms and results in a *uniform* expansion. This method implements a *dynamical renormalization group* resummation which was already implemented successfully to non-equilibrium evolution in quantum field theory [29] and previously applied to quantum mechanical problems [30,31].

In this section we implement the method of multitime scales to the equations for the expectation value and the *q-modes* which we write in the form

$$\left[\frac{d^2}{d\tau^2}+q^2+\mathcal{M}^2(\tau)\right]\varphi_q(\tau)=0 \tag{4.44}$$

$$\left[\frac{d^2}{d\tau^2}+\mathcal{M}^2(\tau)\right]\eta(\tau)=0 \tag{4.45}$$

and use the asymptotic behavior of the effective mass squared obtained from the detailed numerical analysis $\mathcal{M}^2(\tau)$ for $\tau>\tau_1$:

$$\mathcal{M}^2(\tau)=\mathcal{M}_\infty^2+\frac{p_1(\tau)}{\tau}+\mathcal{O}\left(\frac{1}{\tau^2}\right) \tag{4.46}$$

$$p_1(\tau)=K_1\cos[2\mathcal{M}_\infty\tau+2a_2\,\ln(\tau/\tau_1)+\gamma_1] +K_2\cos[2\mathcal{M}_0\tau+2b_2\,\ln(\tau/\tau_1)+\gamma_2] \tag{4.47}$$

$$\mathcal{M}_\infty^2=1+\frac{\eta_0^2}{2},\quad \mathcal{M}_0^2=1+\eta_0^2$$

with $\tau_1\approx\ln[1/g]$ [see Eq. (3.25)] being the non-linear time scale.

As emphasized above, the non-perturbative dynamics has generated a new time scale τ_1 and for weak coupling there are at least two widely separated time scales, the short time scale corresponding to the oscillatory behavior of $\mathcal{O}(\mathcal{M}_\infty^{-1})$ and the long time scale for non-linear relaxation of the order of τ_1.

In order to implement the multitime scale analysis it is convenient to introduce the small quantity ϵ and the following two time variables (T_0 and T_1) by

$$\epsilon=\frac{1}{\tau_1},\quad T_0=\tau,\quad T_1=\epsilon T_0=\frac{\tau}{\tau_1},$$

$$\frac{d}{d\tau}=D_0+\epsilon D_1,\quad D_n=\frac{d}{dT_n},\quad n=0,1$$

and to write $p_1(\tau)/\tau$ in a manner that displays at once the dependence on the short and long time scales:

$$\frac{p_1(\tau)}{\tau}=\epsilon\Gamma(T_0,T_1)$$

$$\Gamma(T_0,T_1)=\frac{K_1}{T_1}\cos[2\mathcal{M}_\infty T_0+2a_2\,\ln(T_1)+\gamma_1] +\frac{K_2}{T_1}\cos[2\mathcal{M}_0T_0 +2b_2\,\ln(T_1)+\gamma_2]. \tag{4.48}$$

To $\mathcal{O}(\epsilon)$ the multitime scale analysis of the asymptotic time dependence of η, φ_q begins by proposing the following *uniform* perturbative expansion for the solution:

$$\eta(T_0,T_1)=\eta^{(0)}(T_0,T_1)+\epsilon\eta^{(1)}(T_0,T_1)+\cdots$$

$$\varphi_q(T_0,T_1)=\varphi_q^{(0)}(T_0,T_1)+\epsilon\varphi_q^{(1)}(T_0,T_1)+\cdots. \tag{4.49}$$

D. $q=0$ modes: η and $\varphi_{q=0}$

We generically call $f(T_0,T_1)$ both η and $\varphi_{q=0}$. The only difference between these is that whereas η is always real, $\varphi_{q=0}$ is complex; this difference will be accounted for in the final form below. Comparing powers of ϵ, we find the following equations for the $q=0$ modes to first order in ϵ:

$$[D_0^2+\mathcal{M}_\infty^2]f^{(0)}(T_0,T_1)=0$$

$$[D_0^2+\mathcal{M}_\infty^2]f^{(1)}(T_0,T_1)=-[2D_0D_1+\Gamma(T_0,T_1)]\times f^{(0)}(T_0,T_1). \tag{4.50}$$

The solution to Eq. (4.50) is obviously

$$f^{(0)}(T_0,T_1)=A(T_1)e^{i\mathcal{M}_\infty T_0}+B(T_1)e^{-i\mathcal{M}_\infty T_0} \tag{4.51}$$

where for η the reality condition implies $B(T_1)=A^*(T_1)$. If the solution of Eqs. (4.50) is sought in terms of the Green's function of the differential operator on the left hand side, one finds that the term proportional to $\cos[2\mathcal{M}_\infty T_0]$ in $\Gamma(T_0,T_1)$ would give rise to secular terms. Therefore the condition for a uniform expansion requires that the coefficients of these secular terms vanish. This leads to the following differential equations for the dependence of the coefficients on the *long* time scale T_1:

$$D_1A-\frac{iK_1}{4\mathcal{M}_\infty T_1}e^{i2a_2\,\ln(T_1)+i\gamma_1}B=0$$

$$D_1B+\frac{iK_1}{4\mathcal{M}_\infty T_1}e^{-i2a_2\,\ln(T_1)+i\gamma_1}A=0. \tag{4.52}$$

We find the solutions

$$A(T_1)=a_{\pm}e^{(i/2)[2a_2\,\ln(T_1)+\gamma_1]}T_1^{\pm a_1},$$

$$B(T_1)=b_{\pm}e^{-(i/2)[2a_2\,\ln(T_1)+\gamma_1]}T_1^{\pm a_1},$$

$$a_1=\sqrt{\left(\frac{K_1}{4\mathcal{M}_\infty}\right)^2-a_2^2},\quad b_{\pm}=e^{\mp i\delta}a_{\pm},$$

$$\tan\delta=\frac{a_1}{a_2}. \tag{4.53}$$

This solution confirms the *power law* relaxation found numerically and provides the consistency condition

$$K_1^2=16\mathcal{M}_\infty^2(a_1^2+a_2^2).$$

This condition is verified numerically to our level of precision. In addition for weak coupling the numerical evidence gives $a_1^2\ll a_2^2$ [see Eqs. (4.4) and (4.23)], leading to

$$K_1\approx 4\mathcal{M}_\infty a_2. \tag{4.54}$$

The final form of the solution is given by a linear combination of the two independent solutions above, yielding

$$f(T_0,T_1)=T_1^{a_1}C_+\cos\left[\mathcal{M}_\infty T_0+a_2\,\ln(T_1)+\frac{\gamma_1}{2}+\frac{\delta}{2}\right]$$
$$+T_1^{-a_1}C_-\cos\left[\mathcal{M}_\infty T_0+a_2\,\ln(T_1)+\frac{\gamma_1}{2}-\frac{\delta}{2}\right]$$
$$+\mathcal{O}(\epsilon)$$

where for η the coefficient C_- is real and $C_+=0$, whereas they are complex and both $\neq 0$ for $\varphi_{q=0}$. The $\mathcal{O}(\epsilon)$ correction quoted above is *bound* as a function of time as it arises from the perturbative solution without secular terms.

Therefore we quote the final form of the solutions

$$\eta(\tau)=D_0\left(\frac{\tau}{\tau_1}\right)^{-a_1}\cos\left[\mathcal{M}_\infty T_0+a_2\,\ln(T_1)+\frac{\gamma_1}{2}-\frac{\delta}{2}\right]$$

$$\varphi_{q=0}(\tau)=C_+\left(\frac{\tau}{\tau_1}\right)^{a_1}\cos\left[\mathcal{M}_\infty T_0+a_2\,\ln(T_1)+\frac{\gamma_1}{2}+\frac{\delta}{2}\right]$$
$$+C_-\left(\frac{\tau}{\tau_1}\right)^{-a_1}\cos\left[\mathcal{M}_\infty T_0+a_2\,\ln(T_1)+\frac{\gamma_1}{2}-\frac{\delta}{2}\right].$$

In addition, we have checked the constancy of the Wronskian

$$\varphi_{q=0}(\tau)\dot{\varphi}^*_{q=0}(\tau)-\dot{\varphi}_{q=0}(\tau)\varphi^*_{q=0}(\tau)$$
$$=2i$$
$$=\mathcal{M}_\infty\,\sin\,\delta[C_+C_-^*-C_+^*C_-],$$

leading to the conclusion that neither of the coefficients $C_\pm$ can vanish for $\varphi_{q=0}$. It is a matter of straightforward algebra to find that these are indeed solutions of Eqs. (4.44) (for $q=0$) and (4.45) up to terms that fall off faster in time. Furthermore, a *uniform* perturbative expansion in ϵ can now be carried out to the next order.

E. $q\neq 0$ modes

Proposing a uniform ϵ-expansion for the mode functions and keeping only up to $\mathcal{O}(\epsilon)$ we find the equation

$$[D_0^2+2\epsilon D_0D_1+q^2+\mathcal{M}_\infty^2+\epsilon\Gamma(T_0,T_1)][\varphi_q^{(0)}(T_0,T_1)$$
$$+\epsilon\varphi_q^{(1)}(T_0,T_1)]=0. \tag{4.55}$$

Since Γ contains the oscillating factors $\cos[2\mathcal{M}_\infty T_0]$ and $\cos[2\mathcal{M}_0T_0]$, a naive perturbative expansion in ϵ will produce secular terms for $\omega_q\approx\mathcal{M}_\infty,\ \mathcal{M}_0$, i.e. for $q\approx 0,\ \mathcal{M}_\infty^2-\mathcal{M}_0^2=\eta_0^2/2$; these were the values for which the resonant denominators in the perturbative expansion vanish. Therefore for these values of q we must implement a multi-time-scale analysis to resum the secular terms.

1. Small but nonzero q^2

A consistent expansion in ϵ can be implemented by writing $q^2=\epsilon q_1^2$ with $q_1\approx\mathcal{O}(1)$. This is a nonrelativistic approximation since then q^2 is much smaller than $\mathcal{M}_\infty^2$. The zeroth order solution is clearly

$$\varphi_q^{(0)}(T_0,T_1)=\mathcal{A}_q(T_1)e^{i\mathcal{M}_\infty T_0}+\mathcal{B}_q(T_1)e^{-i\mathcal{M}_\infty T_0}.$$

Secular terms in a naive perturbative expansion will arise from the term proportional to K_1 in $p_1(\tau)$.

It is convenient to define the coefficients

$$a_q(T_1)=e^{-i[a_2\,\ln(T_1)+(1/2)\gamma_1]}\mathcal{A}_q(T_1),$$

$$b_q(T_1)=e^{i[a_2\,\ln(T_1)+(1/2)\gamma_1]}\mathcal{B}_q(T_1). \tag{4.56}$$

Requesting that the coefficients of the secular terms in the perturbative solution vanish we obtain the following differential equations:

$$D_1a_q+\frac{ia_2a_q}{T_1}-\frac{iq_1^2}{2\mathcal{M}_\infty}a_q-\frac{iK_1}{4\mathcal{M}_\infty T_1}b_q=0$$

$$D_1b_q-\frac{ia_2b_q}{T_1}+\frac{iq_1^2}{2\mathcal{M}_\infty}b_q+\frac{iK_1}{4\mathcal{M}_\infty T_1}a_q=0.$$

These equations simplify considerably by introducing the variable z as

$$z\equiv\frac{q^2T_1}{2\mathcal{M}_\infty}. \tag{4.57}$$

Then, Eqs. (4.56) can be rewritten as two decoupled second order differential equations:

$$\left[z\frac{d^2}{dz^2}+\frac{d}{dz}+z-i-2a_2-\frac{a_1^2}{z}\right]a_q(z)=0 \tag{4.58}$$

$$\left[z\frac{d^2}{dz^2}+\frac{d}{dz}+z+i-2a_2-\frac{a_1^2}{z}\right]b_q(z)=0.$$

These are confluent hypergeometric equations with the solutions

$$\mathcal{A}_q(z)=z^{ia_2-1/2}M_{ia_2-1/2,\pm a_1}(2iz),$$

$$\mathcal{B}_q(z)=z^{-ia_2-1/2}M_{-ia_2-1/2,\pm a_1}(2iz) \qquad (4.59)$$

where $M_{\lambda,\mu}(z)$ stands for a Whittaker function [32]. We find the asymptotic behavior to be given by [32]

$$\mathcal{A}_q(z) \overset{z\to 0}{=} (2i)^{1/2\pm a_1}z^{ia_2\pm a_1},$$

$$\mathcal{B}_q(z) \overset{z\to 0}{=} (2i)^{1/2\pm a_1}z^{-ia_2\pm a_1},$$

and

$$\mathcal{A}_q(z) \overset{z\to\infty}{=} (2i)^{-ia_2+1/2}\frac{\Gamma(1\pm 2a_1)}{\Gamma(1-ia_2\pm a_1)}e^{iz},$$

$$\mathcal{B}_q(z) \overset{z\to\infty}{=} (2i)^{ia_2+1/2}\frac{\Gamma(1\pm 2a_1)}{\Gamma(1+ia_2\pm a_1)}e^{-iz}.$$

In Fig. 14 we plot $|\mathcal{A}_q(z)|$ and the phase of $e^{-iz}\mathcal{A}_q(z)$ as a function of z. One sees that the behavior of the numerically computed modes in Figs. 8(c), 8(d), 9(c) and 9(d) is accurately reproduced.

Using the integral representation for the solutions [32], we can find where the functions $\mathcal{A}_q(z)$ and $\mathcal{B}_q(z)$ oscillate with z and where they do not:

$$\mathcal{A}_q(z)=kz^{ia_2\pm a_1}\int_0^1\frac{dt}{t}e^{i\{2zt+a_2\log[(1-t)/t]\}}[t(1-t)]^{\pm a_1}$$

where k is a constant. This integral has stationary points at

$$t=\frac{1}{2}\left[1\pm\sqrt{1-\frac{2a_2}{z}}\right].$$

For $z>2a_2$ the stationary points are real, indicating an oscillatory behavior, whereas they are complex for $z<2a_2$, implying a non-oscillatory behavior. We see from Eqs. (4.57) and (4.54) that the condition $z=2a_2$ precisely corresponds to the peak position (4.6).

2. $q^2\approx\mathcal{M}_0^2-\mathcal{M}_\infty^2$

In this region of momentum we write $q^2=\mathcal{M}_0^2-\mathcal{M}_\infty^2+\epsilon q_2^2$ in order to implement a multi-time-scale analysis. In this case, secular terms in the perturbative expansion in ϵ will arise from the term proportional to K_2 in $p_1(\tau)$, i.e. the term $\cos[2\mathcal{M}_0T_0]$.

Using the same notation as in the previous subsection, the zeroth order solution is now

$$\varphi_q^{(0)}(T_0,T_1)=\mathcal{A}_q(T_1)e^{i\mathcal{M}_0T_0}+\mathcal{B}_q(T_1)e^{-i\mathcal{M}_0T_0}. \qquad (4.60)$$

Defining the coefficients

$$a_q(T_1)=e^{-(i/2)[2b_2\ln(T_1)+\gamma_2]}\mathcal{A}_q(T_1)$$

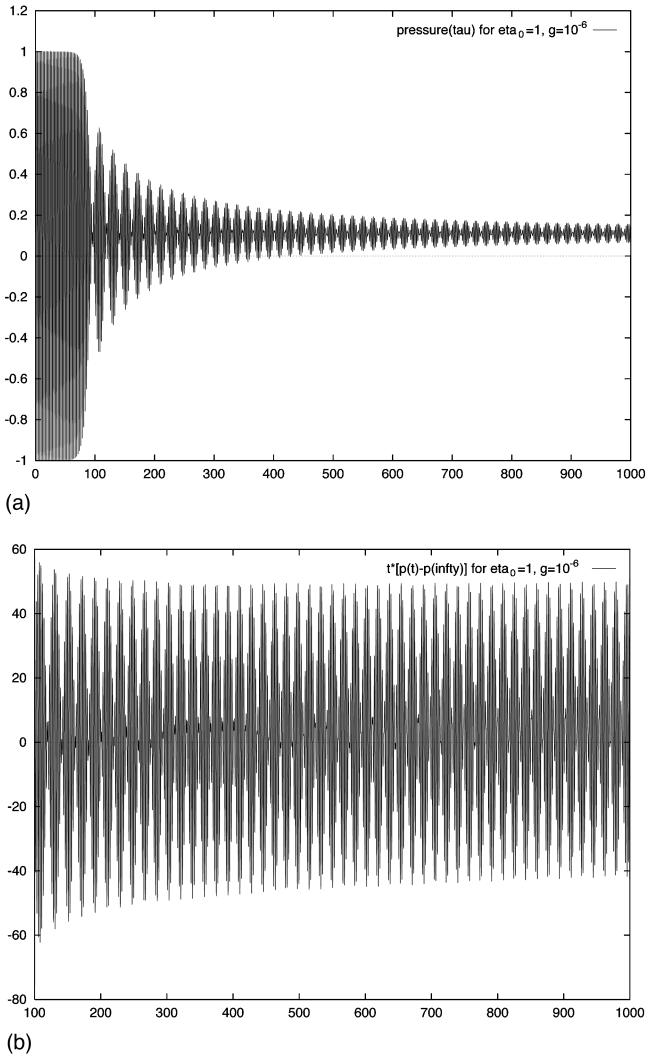

FIG. 14. (a) The pressure divided by the initial energy as a function of time for $\eta_0=1$, $g=10^{-6}$. Notice the asymptotic value $p(\infty)/\varepsilon\approx 1/3(1+2/\eta_0^2)=1/9$. (b) The pressure minus its value at $\tau=\infty$ times τ as a function of time for $\eta_0=1$, $g=10^{-6}$. This function oscillates in time with constant amplitude and frequencies $2\mathcal{M}_\infty=2\sqrt{1+\eta_0^2/2}$ and $2\mathcal{M}_0=2\sqrt{1+\eta_0^2}$.

$$b_q(T_1)=e^{(i/2)[2b_2\ln(T_1)+\gamma_2]}\mathcal{B}_q(T_1).$$

Requesting that the coefficients of the secular terms in the perturbative solution vanish we obtain the following differential equations:

$$D_1a_q+ib_2\frac{a_q}{T_1}-i\frac{q_2^2}{2\mathcal{M}_0}a_q-i\frac{K_2}{4\mathcal{M}_0T_1}b_q=0$$

$$D_1b_q-ib_2\frac{b_q}{T_1}+i\frac{q_2^2}{2\mathcal{M}_0}b_q+i\frac{K_2}{4\mathcal{M}_0T_1}a_q=0.$$

As in the previous case these coupled first order differential equations reduce to two decoupled confluent hypergeometric equations with solution

$$\mathcal{A}_q(y)=y^{ib_2-1/2}M_{ib_2-1/2,\pm b_1}(2iy),$$

$$\mathcal{B}_q(y)=y^{-ib_2-1/2}M_{-ib_2-1/2,\pm b_1}(2iy)$$

where

$$y\equiv\frac{(\eta_0^2/2-q^2)}{2\mathcal{M}_0}\tau.$$

The transition from non-oscillatory to oscillatory behavior takes place here at $y=2b_2$, implying that the modes with

$$q^2<\frac{\eta_0^2}{2}-\frac{4b_2\mathcal{M}_0}{\tau}$$

will grow in time.

The solutions for the mode with $q=\eta_0/\sqrt{2}$ correspond to the exponents

$$\varphi_{q=\frac{\eta}{\sqrt{2}}}=\tau^{\pm b_1+ib_2}$$

$$b_1=\sqrt{\left(\frac{K_2}{4\mathcal{M}_0}\right)^2-b_2^2}.$$

This analysis leads to the conclusion that as a consistency condition, the constants K_1 and K_2 can be expressed as follows:

$$K_1\approx 4\sqrt{1+\eta_0^2/2}(0.16\ \log g^{-1}+0.6),$$

$$K_2\approx 4\sqrt{1+\eta_0^2}\times(-0.16\ \log g^{-1}+0.6), \tag{4.61}$$

where we used Eqs. (4.4), (4.23) and (4.28).

Therefore the effective mass squared behaves as

$$\mathcal{M}^2(\tau)=\mathcal{M}_\infty^2+\frac{4}{\tau}\{\mathcal{M}_\infty a_2\ \cos[2\mathcal{M}_\infty\tau+2a_2\ \log(\tau/\tau_1)+\gamma_1]+\mathcal{M}_0 b_2\cos[2\mathcal{M}_0\tau+2b_2\ \log(\tau/\tau_1)+\gamma_2]\}+\mathcal{O}\left(\frac{1}{\tau^2}\right).$$

We have confirmed these results numerically within our precision.

These results are noteworthy; by implementing a multi-time scale analysis which is the dynamical equivalent of a renormalization group resummation [29] we have obtained a power law relaxation for the expectation value with *non-universal dynamical anomalous dimensions*. The logarithmic phases are clearly a consequence of the $1/\tau$ falloff of the potential $w(\tau)$ in the mode equations (4.33) just as in the Coulomb problem. The power laws originate from the resummation of the secular terms arising from the non-linear resonances, a non-perturbative result.

F. Energy and pressure

The energy-momentum tensor for this theory in Minkowski spacetime is given by

$$T^{\mu\nu}=\partial^\mu\vec{\Phi}\cdot\partial^\nu\vec{\Phi}-g^{\mu\nu}\left[\frac{1}{2}\partial_\alpha\vec{\Phi}\cdot\partial^\alpha\vec{\Phi}-V(\vec{\Phi}\cdot\vec{\Phi})\right]. \tag{4.62}$$

Since we consider translationally as well as rotationally invariant states, the expectation value of $T^{\mu\nu}$ takes the fluid form

$$E=\frac{1}{N\mathcal{V}}\langle T^{00}(x)\rangle=\frac{1}{N\mathcal{V}}\left\langle\frac{1}{2}\dot{\vec{\Phi}}^2+\frac{1}{2}(\nabla\vec{\Phi})^2+V(\Phi)\right\rangle$$

$$N\mathcal{V}P(\tau)=\langle T^{11}(x)\rangle=\langle T^{22}(x)\rangle=\langle T^{33}(x)\rangle=\left\langle\frac{1}{3}(\nabla\vec{\Phi})^2+\dot{\vec{\Phi}}^2-T^{00}(x)\right\rangle,$$

with all off-diagonal components vanishing.

Hence,

$$P(\tau)+E=\frac{1}{N\mathcal{V}}\left\langle\frac{1}{3}(\nabla\vec{\Phi})^2+\dot{\vec{\Phi}}^2\right\rangle$$

takes a particularly simple form.

Both E and $P(\tau)+E$ can be expressed in terms of the zero mode and the q-modes. All derivations including the renormalization procedure can be found in Refs. [20,27,33]. We just quote the final results in the unbroken symmetry case, referring the reader to the above references for details:

$$E_{ren}=\frac{2|M_R|^4}{\lambda_R}\left\{\frac{1}{2}\dot{\eta}^2+\frac{1}{2}(1+\eta^2)\mathcal{M}^2(\tau)-\frac{\mathcal{M}^4(\tau)+1}{4}+g\left[\varepsilon_F(\tau)+\frac{1}{2}J^+(\eta_0)\mathcal{M}^2(\tau)+\frac{\mathcal{M}^4(\tau)}{32}+\frac{\mathcal{M}^4(\tau)}{8}\ln\left(\frac{1}{2}\mathcal{M}(\tau)\right)+\mathcal{C}^+(\eta_0)\right]\right\}, \tag{4.63}$$

where [20,27]

$$\varepsilon_F(\tau)=2\int_0^\infty q^2dq\,\omega_q(\tau)N_q^{ad}(\tau)$$

$$J^+(\eta_0)=-\frac{1+\eta_0^2}{4}\left[1+\log\left(\frac{1+\eta_0^2}{4}\right)\right]$$

$$\mathcal{C}^+(\eta_0)=-\frac{3}{4}(1+\eta_0^2)J^+(\eta_0).$$

Since energy is conserved (as can be verified explicitly by using the equations of motion), it is equal to the initial value, given by

$$E_{ren}=\frac{2|M_R|^4}{\lambda_R}\varepsilon=\frac{2|M_R|^4}{\lambda_R}\left\{\frac{1}{2}\eta_0^2\left[1+\frac{1}{2}\eta_0^2\right]\right\}. \tag{4.64}$$

The renormalized energy plus pressure takes the form [20,27]

$$P(\tau)_{ren}+E_{ren}=\frac{2|M_R|^4}{\lambda_R}[\varepsilon+p(\tau)]$$

$$=\frac{2|M_R|^4}{\lambda_R}\Bigg\{\dot{\eta}^2+g\int_0^\infty q^2dq \times\Bigg(\left|\dot{\varphi}_q(\tau)\right|^2+\frac{1}{3}q^2\left|\varphi_q(\tau)\right|^2 -\frac{4}{3}q-\frac{\mathcal{M}^2(\tau)}{3q} +\frac{\theta(q-K)}{12q^3}\frac{d^2}{d\tau^2}[\mathcal{M}^2(\tau)]\Bigg)\Bigg\}.$$

For times after τ_1 we can restrict ourselves to the contribution from the expectation value η and the modes in the band $0<q<\eta_0/\sqrt{2}$. Modes with $q>\eta_0/\sqrt{2}$ only yield perturbatively small corrections $\mathcal{O}(g)$. Using Eq. (4.11) we can write the integrands in Eqs. (4.63)–(4.65) as follows:

$$g|\varphi_q(\tau)|^2=M_q(\tau)^2\{1+\cos[2\omega(q)\tau+\phi_q(\tau)]\}[1+O(g)],$$

$$g|\dot{\varphi}_q(\tau)|^2=\omega(q)^2M_q(\tau)^2\{1-\cos[2\omega(q)\tau+\phi_q(\tau)]\} \times[1+O(g)].$$

Inserting these expressions in Eqs. (4.63)–(4.65) yields

$$\varepsilon=\frac{1}{2}\dot{\eta}^2+\frac{1}{2}(1+\eta^2)\mathcal{M}^2(\tau)-\frac{\mathcal{M}^4(\tau)+1}{4} +\int_0^{\eta_0/\sqrt{2}}q^2dq[q^2+\mathcal{M}^2(\infty)]M_q(\tau)^2+\mathcal{O}(g).$$

Taking now the $\tau\to\infty$ limit yields

$$\varepsilon=-\frac{1}{16}\eta_0^4+\int_0^{\eta_0/\sqrt{2}}q^2dq[q^2+\mathcal{M}^2(\infty)]M_q(\infty)^2+\mathcal{O}(g). \tag{4.65}$$

We analogously find, for $\varepsilon+p(\tau)$,

$$\varepsilon+p(\tau)=\int_0^{\eta_0/\sqrt{2}}q^2dq\left[\frac{4}{3}q^2+\mathcal{M}^2(\infty)\right]M_q(\tau)^2 -\int_0^{\eta_0/\sqrt{2}}q^2dq\,\cos[2\omega(q)\tau+\phi_q(\tau)] \times\left[\frac{2}{3}q^2+\mathcal{M}^2(\infty)\right]M_q(\tau)^2+\mathcal{O}(g).$$

For large τ the integral containing the oscillating cosinus dies off. We thus obtain, combining both expressions,

$$p(\infty)=\frac{1}{3}\int_0^{\eta_0/\sqrt{2}}q^4dqM_q(\infty)^2+\frac{1}{16}\eta_0^4+\mathcal{O}(g). \tag{4.66}$$

G. Sum rules and the equation of state

Although we do not know the analytic form of the particle distribution for late times [see Eq. (4.29)], we are able to compute its first two moments in the following way.

First, we can express the quantum fluctuations $g\Sigma(\tau)$ in terms of the modes using Eqs. (3.7) and (4.18):

$$g\Sigma(\tau)=\int_0^{\eta_0/\sqrt{2}}q^2dqM_q(\tau)^2\{1+\cos[2\omega(q)\tau+\phi_q(\tau)]\} +\mathcal{O}(g).$$

For large τ the integral containing the oscillating cosinus dies off. Using now that $\eta(\infty)=0$, $\mathcal{M}^2(\tau)=1+\eta(\tau)^2+g\Sigma(\tau)$ and Eq. (4.1) we obtain the first sum rule

$$\int_0^{\eta_0/\sqrt{2}}q^2dqM_q(\infty)^2=\frac{1}{2}\eta_0^2+\mathcal{O}(g).$$

Furthermore, equating the expression for the energy for $\tau=\infty$ [Eq. (4.65)] with its initial value [Eq. (4.64)] yields the second sum rule

$$\int_0^{\eta_0/\sqrt{2}}q^4dqM_q(\infty)^2=\frac{1}{16}\eta_0^4+\mathcal{O}(g).$$

Combining the sum rules with the expressions for the energy and pressure, Eqs. (4.65) and (4.66), yields

$$p(\infty)=\frac{1}{12}\eta_0^4+\mathcal{O}(g)$$

and

$$\frac{p(\infty)}{\varepsilon}=\frac{1}{3\left(1+\frac{2}{\eta_0^2}\right)}+\mathcal{O}(g).$$

We see that the bath of produced particles does not behave asymptotically either as radiation or as nonrelativistic matter but their equation of state interpolates between these two limits as a function of the initial amplitude of η.

For large η_0, we find, as expected, radiation behavior

$$\frac{p(\infty)}{\varepsilon}\overset{\eta_0\to\infty}{=}\frac{1}{3}+\mathcal{O}\left(\frac{1}{\eta_0^2}\right).$$

For small η_0, we find a cold matter behavior

$$\frac{p(\infty)}{\varepsilon}\overset{\eta_0\to 0}{=}\frac{1}{6}\eta_0^2+\mathcal{O}(\eta_0^4)\to 0.$$

We notice that the energy and the asymptotic pressure can be expressed in a form that suggests a two component fluid formed by nonrelativistic and massless particles:

$$p(\infty)=0\times\frac{\eta_0^2}{2}+\frac{1}{3}\frac{\eta_0^4}{4}$$

$$\varepsilon=\frac{\eta_0^2}{2}+\frac{\eta_0^4}{4}.$$

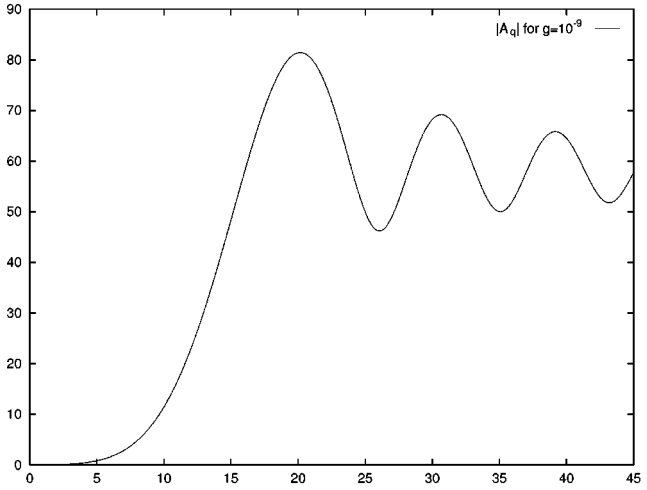

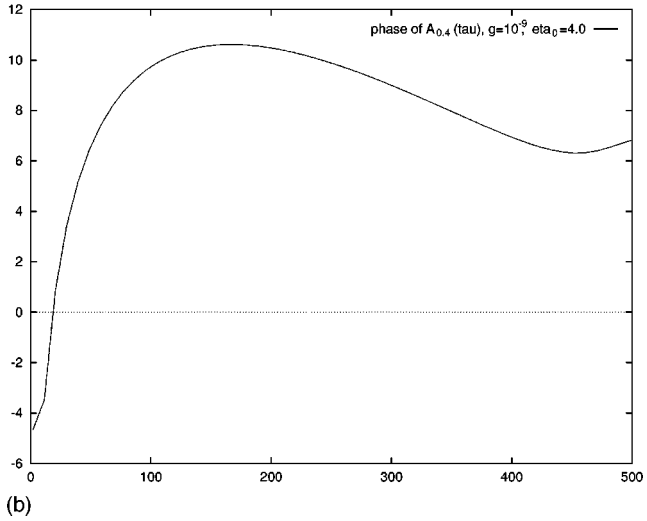

FIG. 15. (a) Modulus of the function $\mathcal{A}_q(T_1)$ obtained through multi-time-scale analysis as a function of $q^2\tau/\mathcal{M}_\infty$. We give in Eq. (4.59) its expression in terms of Whittaker functions. Notice the resemblance with the full numerical solutions displayed in Figs. 8(c) and 8(d). (b) Phase of the function $\mathcal{A}_q(T_1)$ obtained through multi-time-scale analysis as a function of $q^2\tau/\mathcal{M}_\infty$. We give in Eq. (4.59) its expression in terms of Whittaker functions. Notice the resemblance with the full numerical solutions displayed in Figs. 9(c) and 9(d).

$\eta_0^2/2$ and $\eta_0^4/4$ may be interpreted as the contributions of massless and massive particles to the total energy.

The pressure approaches its asymptotic limit $p(\infty)$, oscillating with decreasing amplitude. We find from our numerical analysis [see Figs. 15(a) and 15(b)] that this amplitude falls off as $\sim 1/\tau$. More precisely we find, for times later than τ_1,

$$p(\tau)=p(\infty)+\frac{q_1(\tau)}{\tau}+\mathcal{O}\left(\frac{1}{\tau^2}\right).$$

Here, $q_1(\tau)$ oscillates with time with the same frequencies $2\mathcal{M}_\infty$ and $2\mathcal{M}_0$ as the effective mass squared [see Eq. (4.3)].

V. BROKEN SYMMETRY

In the case of broken symmetry $M_R^2=-|M_R^2|$ and the field equations in the $N=\infty$ limit become [20,27,34]

$$\ddot{\eta}-\eta+\eta^3+g\,\eta(\tau)\Sigma(\tau)=0 \tag{5.1}$$

$$\left[\frac{d^2}{d\tau^2}+q^2-1+\eta(\tau)^2+g\Sigma(\tau)\right]\varphi_q(\tau)=0 \tag{5.2}$$

where $\Sigma(\tau)$ is given in terms of the mode functions $\varphi_q(\tau)$ by the same expression of the previous case, Eq. (3.7). Here, $\mathcal{M}^2(\tau)\equiv-1+\eta(\tau)^2+g\Sigma(\tau)$ plays the role of a (time dependent) renormalized effective mass squared.

The choice of boundary conditions is more subtle for broken symmetry. The situation of interest is when $0<\eta_0^2\ll 1$, corresponding to the situation where the expectation value rolls down the potential hill, beginning very close to the origin. The modes with $q^2<1-\eta_0^2$ are unstable and thus do not represent simple harmonic oscillator quantum states. Therefore one *must* choose a different set of boundary conditions for these modes. Our choice will be that corresponding to the ground state of an *upright* harmonic oscillator. This particular initial condition corresponds to a quench type of situation in which the initial state is evolved in time in an inverted parabolic potential (for early times $t>0$). Thus we shall use the following initial conditions for the mode functions:

$$\varphi_q(0)=\frac{1}{\sqrt{\Omega_q}},\quad \dot{\varphi}_q(0)=-i\sqrt{\Omega_q}, \tag{5.3}$$

$$\Omega_q=\sqrt{q^2+1+\eta_0^2}\quad \text{for}\quad q^2<q_u^2\equiv 1-\eta_0^2,$$

$$\Omega_q=\sqrt{q^2-1+\eta_0^2}\quad \text{for}\quad q^2>q_u^2,\quad 0\leqslant\eta_0^2<1. \tag{5.4}$$

along with the initial conditions for the expectation value given by Eq. (3.3). Furthermore, because the adiabatic frequencies cannot be defined for the modes in the spinodal band, we use the definition, Eq. (3.8), for the particle number.

A. Early time evolution: Spinodal unstabilities

As in the unbroken case, for $g\ll 1$ we can neglect $g\Sigma(\tau)$ in Eqs. (5.1),(5.2) until the spinodal time τ_1 defined to be the time scale at which the quantum fluctuations become comparable to the ''tree level'' terms. In addition, when the initial value of η_0 is zero or much smaller than 1, we can neglect $\eta(\tau)^2$ in the mode equations, which simplify to

$$\left[\frac{d^2}{d\tau^2}+q^2-1\right]\varphi_q(\tau)=0. \tag{5.5}$$

The solution of Eqs. (5.5) for the initial conditions (5.3) takes the form

$$\varphi_q(\tau)=\frac{1}{2\sqrt{1-q^4}}\{[\sqrt{1-q^2}-i(1+q^2)]e^{\tau\sqrt{1-q^2}}$$

TABLE I. Spinodal time estimates from the analytic formula (5.8) compared with the numerical results for different values of the coupling $g=10^{-n}$.

$n=-\log_{10}g$	Spinodal time (τ_1) estimate	Numerical result for τ_1
5	7.85	7.87
6	9.14	9.14
7	10.40	10.40
8	11.65	11.40
9	12.89	12.87
10	14.14	14.10
12	16.55	16.90
14	19.00	19.29

$$+[\sqrt{1-q^2}+i(1+q^2)]e^{-\tau\sqrt{1-q^2}}\}$$

for $0<q^2<1$. The modes with higher wave number $q^2>1$ do not grow and their contribution to $g\Sigma(\tau)$ is subleading at long times.

This solution exhibits the typical exponential growth of spinodal unstabilities. Very soon, the decreasing exponential can be neglected and we can set

$$\varphi_q(\tau)\approx\frac{1}{2\sqrt{1-q^4}}[\sqrt{1-q^2}-i(1+q^2)]e^{\tau\sqrt{1-q^2}} \quad (5.6)$$

to a very good approximation.

Using such mode functions we can estimate the quantum fluctuations $g\Sigma(\tau)$ for short times. Inserting $\varphi_q(\tau)$ given by Eq. (5.6) in Eq. (3.7) the integral is dominated by $q=0$ for growing times τ:

$$\Sigma(\tau)\approx\frac{1}{2}\int_0^{1-0}\frac{q^2dq}{1-q^4}\left[1+\frac{q^2}{2}(1+q^2)\right]e^{2\tau\sqrt{1-q^2}}$$
$$\approx\frac{\sqrt{\pi}}{8\tau^{3/2}}e^{2\tau}\left[1+\mathcal{O}\left(\frac{1}{\tau}\right)\right]. \quad (5.7)$$

Using this estimate for the quantum fluctuations $\Sigma(\tau)$, we can now find the value of the spinodal time scale τ_1 at which the back reaction becomes comparable to the classical terms in the differential equations. Such a time is defined by $g\Sigma(\tau_1)\sim 1$. From the results presented above, we find

$$\tau_1\approx\frac{1}{2}\log\left[\sqrt{\frac{8}{\pi}}\frac{1}{g}\right]+\frac{3}{4}\log\log\left[\frac{8}{\sqrt{\pi}g}\right]+\cdots. \quad (5.8)$$

The time interval from $\tau=0$ to $\tau\sim\tau_1$ is when most of the particle production takes place. After $\tau\sim\tau_1$ the quantum fluctuation shut off the exponential growth of the modes and particle production slows down dramatically.

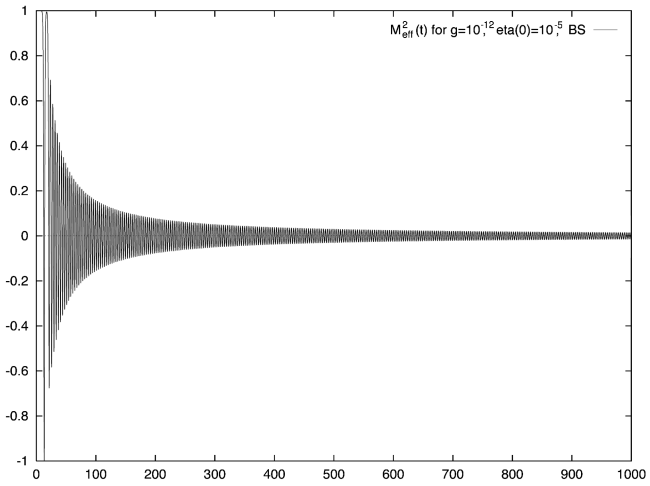

FIG. 16. The effective mass squared as a function of time for broken symmetry $\eta_0=10^{-5}$, $g=10^{-12}$. This function oscillates in time as described by Eq. (5.10).

We list in Table I the values of the spinodal time according to Eq. (5.8) and the corresponding position of the maximum of $g\Sigma(\tau)$ for different values of $g=10^{-n}$ and a fixed $\eta_0=10^{-4}$. We see that the two values are equal up to 2%.

B. Asymptotic nonlinear evolution I: Numerical analysis

We present in this section the numerical analysis for the time evolution *after* the spinodal time τ_1 when the quantum back reaction from $g\Sigma(\tau)$ becomes important and a full solution of the non-linear equations (5.1), (5.2) is required. We have carried out a numerical integration of the integro-differential equations for a wide range of initial amplitudes and couplings, implementing the same algorithms and with the same precision as in the unbroken symmetry case before. In the broken symmetry case we find numerically that the effective mass squared

$$\mathcal{M}^2(\tau)\equiv-1+\eta(\tau)^2+g\Sigma(\tau) \quad (5.9)$$

vanishes for $\tau\to\infty$.

A detailed analysis that includes the FFT reveals that $\mathcal{M}^2(\tau)$ tends to zero, oscillating with decreasing amplitude. For $\tau>\tau_1$ a very precise fit is obtained in the form (see Fig. 16)

$$\mathcal{M}^2(\tau)=\frac{A}{\tau}s(\tau)\cos\left[2\tau+2c_2s(\tau)\log\left(\frac{\tau}{\tau_1}\right)+\gamma\right]+\mathcal{O}\left(\frac{1}{\tau^2}\right) \quad (5.10)$$

where A, c_2 and γ are constants and $s(\tau)$ is a slowly decreasing function with $s(\tau_1)\approx 1$. This slowly varying function can be well approximated by

$$s(\tau)\approx e^{-(\tau/\tau_2)^x}. \quad (5.11)$$

For small initial amplitudes ($\eta_0<10^{-3}$), A and τ_0 are independent of η_0 and their dependence on g can be numerically fit as follows:

$$x \approx 0.25, \quad \tau_0 \sim 1/\sqrt{g}, \quad A \approx 0.64 \log\frac{1}{g} - 1.9,$$

$$c_2 \approx 0.6 - 0.16 \log\frac{1}{g} \tag{5.12}$$

for small couplings ($g < 10^{-4}$).

These expressions reveal that a *second* dynamical time scale τ_2 emerges in the broken symmetry case. Furthermore, this new scale is widely separated from the non-linear scale, i.e. $\tau_2 \gg \tau_1$ for weak coupling and small initial amplitude.

We also notice that the frequency of the oscillation of the effective mass is given by the initial mass (for very small η_0), which is in agreement with the situation in the unbroken phase [see Eq. (4.3)] since in this broken symmetry case the effective mass vanishes asymptotically.

A power law relaxation was also reported in [34] for the broken symmetry phase.

C. Evolution of the mode functions

Since the effective mass vanishes asymptotically, the q-modes $\varphi_q(\tau)$ oscillate as

$$\varphi_q(\tau) \overset{\tau\to\infty}{=} A_q e^{iq\tau} + B_q e^{-iq\tau} + \mathcal{O}\left(\frac{1}{\tau}\right), \tag{5.13}$$

behavior that is confirmed in our numerical analysis.

As for the unbroken symmetry case, it is convenient to introduce slowly varying amplitudes $A_q(\tau)$ and $B_q(\tau)$,

$$A_q(\tau) \equiv \frac{1}{2} e^{-iq\tau}\left[\varphi_q(\tau) - \frac{i}{q}\dot{\varphi}_q(\tau)\right],$$

$$B_q(\tau) \equiv \frac{1}{2} e^{+iq\tau}\left[\varphi_q(\tau) + \frac{i}{q}\dot{\varphi}_q(\tau)\right], \tag{5.14}$$

to separate the evolution on short time scales from that on the long time scales. We can thus express the mode functions $\varphi_q(\tau)$ in terms of $A_q(\tau)$ and $B_q(\tau)$ as follows:

$$\varphi_q(\tau) = A_q(\tau) e^{iq\tau} + B_q(\tau) e^{-iq\tau}. \tag{5.15}$$

We find, from Eqs. (5.13), (5.14),

$$\lim_{\tau\to\infty} A_q(\tau) = A_q, \tag{5.16}$$

$$\lim_{\tau\to\infty} B_q(\tau) = B_q. \tag{5.17}$$

We obtain, from Eq. (5.14) for the square modulus of the modes,

$$|\varphi_q(\tau)|^2 = |A_q(\tau)|^2 + |B_q(\tau)|^2 + 2|A_q(\tau) B_q(\tau)| \times \cos[2q\tau + \phi_q(\tau)] \tag{5.18}$$

where we set

$$A_q(\tau) B_q(\tau)^* = |A_q(\tau) B_q(\tau)| e^{i\phi_q(\tau)}. \tag{5.19}$$

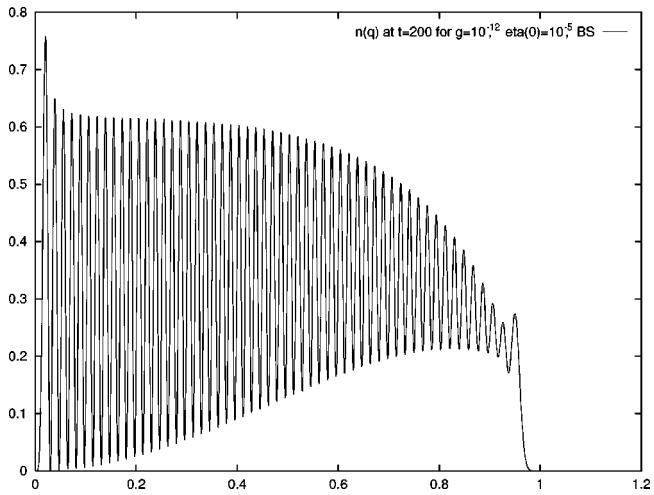

FIG. 17. Momentum distribution of the produced particles at $\tau = 200$ for broken symmetry $\eta_0 = 10^{-5}$, $g = 10^{-12}$. Notice the main peak at $q = 0.020$ and the secondary peak at $q = 0.946$ associated with the non-linear resonance at $q = 1$. The positions of both peaks are correctly estimated by Eqs. (5.23) and (5.24), respectively.

The Wronskian relation (3.6) and Eq. (5.13) imply that the functions $A_q(\tau)$ and $B_q(\tau)$ are related through

$$|B_q(\tau)|^2 - |A_q(\tau)|^2 = \frac{1}{q} \tag{5.20}$$

plus terms that vanish fast asymptotically. We plot in Figs. 17 and 18 the (scaled) modulus as a function of time,

$$M_q(\tau) \equiv \sqrt{g}\sqrt{|A_q(\tau)|^2 + |B_q(\tau)|^2}, \tag{5.21}$$

and $\phi_q(\tau)$ for some relevant cases. This figure shows that as anticipated, $M_q(\tau)$ and $\phi_q(\tau)$ vary *slowly* with τ.

For small coupling g, $|\varphi_q(\tau)|^2, |B_q(\tau)|^2$ and $|A_q(\tau)|^2$ are of order $1/g$ for q in the spinodal band $0 \leqslant q \leqslant 1$ and times later than τ_1 [20,27]. Therefore, $M_q(\tau)$ is in that case of order one. Moreover, Eq. (5.20) implies that $|B_q(\tau)|^2 = |A_q(\tau)|^2[1 + O(g)]$ and we can approximate Eq. (5.18) as follows:

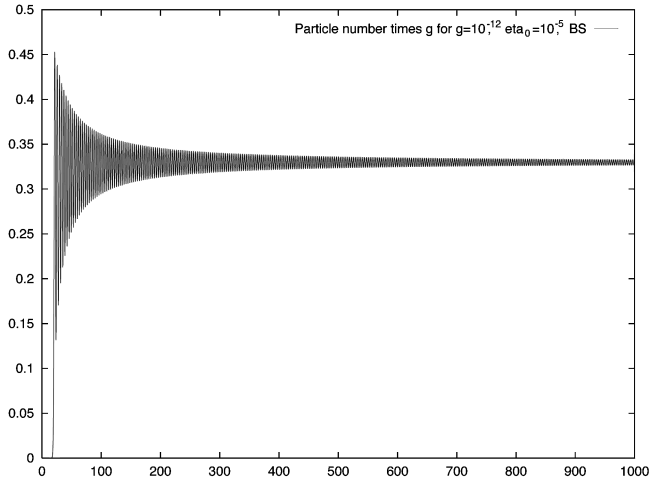

FIG. 18. The total occupation number times g per volume m^{-3} as a function of time for broken symmetry, $\eta_0 = 10^{-5}$, $g = 10^{-12}$. Its limiting value is $g\mathcal{N}(\infty) \approx 0.33$.

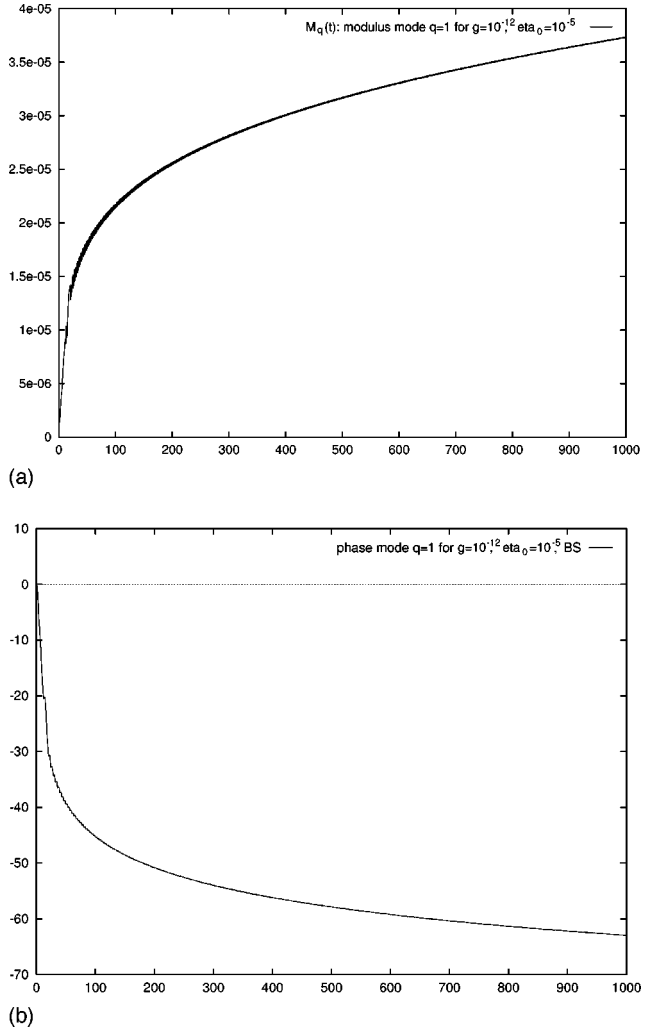

FIG. 19. (a) The amplitude $M_q(\tau)$ of the mode function $\varphi_{q=1}(\tau)$ as a function of time for broken symmetry, $\eta_0=10^{-5}$, $g=10^{-12}$. It grows as a power according to Eq. (5.26). (b) The phase $\phi_q(\tau)$ of the mode function $\varphi_{q=1}(\tau)$ as a function of time for broken symmetry, $\eta_0=10^{-5}$, $g=10^{-12}$. This function follows Eq. (5.26) with a very good approximation.

$$g|\varphi_q(\tau)|^2=M_q(\tau)^2\{1+\cos[2q\tau+\phi_q(\tau)]\}[1+O(g)], \tag{5.22}$$

for $0<q<1$.

We see from the numerical results (Fig. 19) that the momentum distribution of produced particles evolves with time. In particular, the position of its peak $q_B(\tau)$ decreases with time. From the numerical results we can fit the peak position by the form

$$q_B(\tau)\approx\frac{r_1}{\tau-\tau_B}, \quad \tau>\tau_1, \tag{5.23}$$

where $r_1\approx 3.8$ for $g<10^{-4}$, $\eta_0<10^{-5}$ and $\tau_B\sim\tau_1$.

Since $\mathcal{M}^2(\infty)=0$, the asymptotic equation for the zero mode, $\ddot{\eta}(\tau)=0$, only admits a constant as bounded solution. This is precisely what the numerical analysis yields.

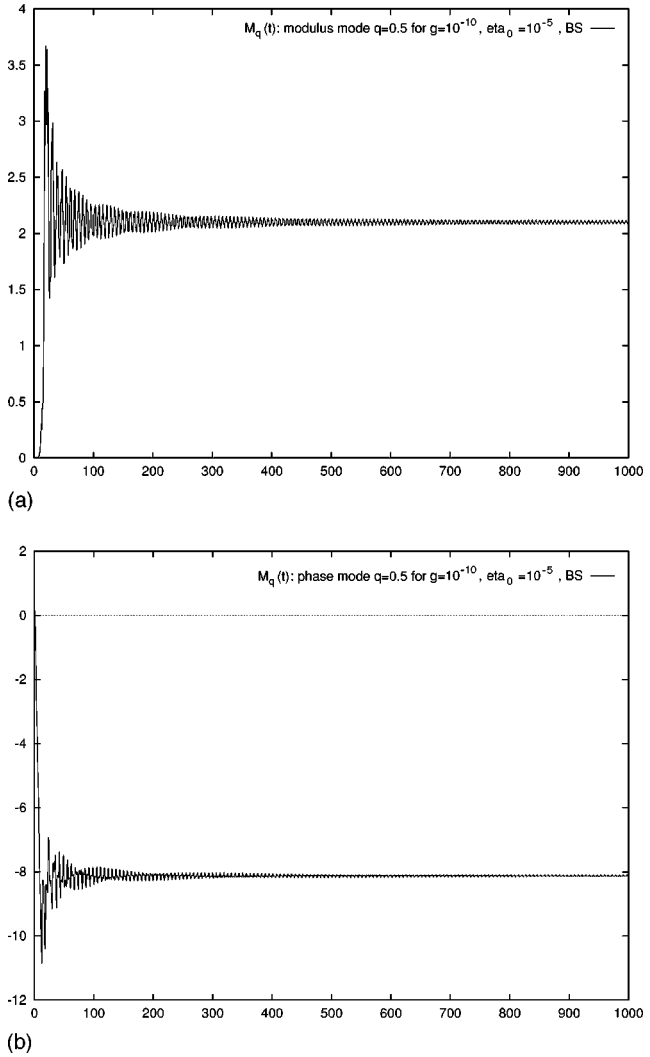

FIG. 20. (a) The modulus $M_q(\tau)$ of the mode function $\varphi_{q=0.5}(\tau)$ as a function of time for $g=10^{-10}$, $\eta_0=10^{-5}$, broken symmetry. For times later than $\tau_1=14.14\ldots$, this mode oscillates with stationary amplitude. It lies outside the nonlinear resonance. (b) The phase $\phi_q(\tau)$ of the mode function $\varphi_{q=0.5}(\tau)$ as a function of time for $g=10^{-10}$, $\eta_0=10^{-5}$, broken symmetry.

We find two non-linear resonant bands for $\tau>\tau_1$, the first for $0<q<q_B(\tau)$ and the second for $q_C(\tau)<q<\sqrt{1-\eta_0^2}\approx 1$. The value of $q_C(\tau)$ follows by perturbation analysis (see the next section):

$$q_C(\tau)\approx 1-\frac{A}{\tau-\tau_C}s(\tau), \quad \tau>\tau_1, \tag{5.24}$$

where $\tau_C\sim\tau_1$.

We see from Eqs. (5.23) and (5.24) that both unstable bands shrink to zero for $\tau\to\infty$. The modes in these nonlinear resonant bands grow as powers of time. The mode exactly at $q=0$ is not resonant. $\eta(\tau)$ tends to a constant value for $\tau\to\infty$ while $\varphi_{q=0}(\tau)$ grows linearly with the time.

The order parameter $\eta(\tau)$ tends for late times to a nonzero limit that depends on the initial conditions.

The modes between the unstable bands $[q_B(\tau)<q<q_C(\tau)]$ oscillate in time with constant amplitude (see Fig. 18).

Most of the particles are produced just before the time τ_1 (see Fig. 20). Then, the particle number oscillates with decreasing amplitude around its asymptotic limit. This limiting value is proportional to g^{-1} and independent of η_0 for small η_0 and g and approximately given by

$$\mathcal{N}(\infty)\approx\frac{0.330}{4\pi^2 g}. \tag{5.25}$$

In the present case the particle number saturates around τ_1.

The vanishing of the effective mass in the $\tau\to\infty$ limit implies that the q-modes become effectively free. As for unbroken symmetry (see Sec. III A), the system tends asymptotically to a limit cycle. All modes oscillate harmonically for large enough times, since for $\tau=\infty$ both unstable bands $[0<q<q_B(\tau)$ and $q_C(\tau)<q<1]$ shrink to zero. In addition, the expectation value tends to a small constant value $\eta(\infty)=\eta_\infty$.

In the present broken symmetry case we find that the mode $q=0$ grows linearly in time, whereas modes with $q=\sqrt{1-\eta_0^2}\approx 1$ grow with a power law for $\tau>\tau_1$ approximately given by

$$\begin{aligned} A_{q=1}(\tau)&\approx\tau^{ic_2}[D_1\tau^{c_1}+D_2\tau^{-c_1}],\\ B_{q=1}(\tau)&\approx\tau^{-ic_2}[D_1'\tau^{c_1}+D_2'\tau^{-c_1}] \end{aligned} \tag{5.26}$$

(see Fig. 17) with

$$c_1\approx 0.24,\quad c_2\approx 0.6-0.16\,\log\frac{1}{g}. \tag{5.27}$$

A more precise numerical fit yields that the dependence of c_1 on g can be bounded by

$$\frac{\Delta c_1}{\Delta\log g^{-1}}<4\times 10^{-3}. \tag{5.28}$$

D. Asymptotic nonlinear evolution II: Perturbative and multitime scale analysis

As in the unbroken symmetry case, we can determine analytically the position of the resonances by performing a perturbative analysis in a similar manner, in terms of the advanced Green's function.

The effective mass $\mathcal{M}^2(\tau)$ vanishes for $\tau\to\infty$ in the broken symmetry case [see Eq. (5.10)]. Because the function $s(\tau)$ varies on even longer time scales of order $1/\sqrt{g}$, we can perform a perturbative expansion on intermediate asymptotic scales, between τ_1 and the much longer time scale associated with $s(\tau)$. In this intermediate asymptotic regime we can consider $s(\tau)$ to be constant.

We can thus study the mode equations

$$\left[\frac{d^2}{d\tau^2}+q^2+\mathcal{M}^2(\tau)\right]\varphi_q(\tau)=0 \tag{5.29}$$

for late times, considering $\mathcal{M}^2(\tau)$ as a small perturbation. That is, we can write the integral equation including the boundary conditions (5.13)

$$\begin{aligned} \varphi_q(\tau)=A_q e^{iq\tau}+B_q e^{-iq\tau}\\ -\int_\tau^\infty d\tau'\,\frac{\sin q(\tau'-\tau)}{q}\mathcal{M}^2(\tau')\varphi_q(\tau'). \end{aligned} \tag{5.30}$$

Iterating this integral equation and using Eq. (5.10) yields, after calculation, if we take the function $s(\tau)$ as a constant,

$$\begin{aligned} \varphi_q(\tau)=A_q e^{iq\tau}+B_q e^{-iq\tau}-\frac{Ae^{-(\tau/\tau_0)^x}}{8\tau}\Bigg\{A_q e^{iq\tau}\left[\frac{e^{i\psi(\tau)}}{q+1}\right.\\ \left.-\frac{e^{-i\psi(\tau)}}{q-1}\right]-B_q e^{-iq\tau}\left[\frac{e^{i\psi(\tau)}}{q-1}-\frac{e^{-i\psi(\tau)}}{q+1}\right]\Bigg\} \end{aligned} \tag{5.31}$$

where $\psi(\tau)=2\tau+2c_2 s(\tau)\log(\tau/\tau_1)+\phi$.

These expressions are singular at $q=\pm 1$, revealing the resonant band below $q=1$. Actually, these singularities disappear when the decrease of $s(\tau)$ with τ is taken into account on time scales $\tau\gg\tau_2$.

Notice that there is no resonance at $q=0$ for broken symmetry.

For $q^2\approx 1$ the perturbative expansion breaks down for the intermediate asymptotic time scales $\tau_1\ll\tau\ll\tau_2$.

In order to understand the behavior of the mode functions in the resonant regions, we implement a multitime scale analysis in the same manner as in the unbroken symmetry case, introducing the parameter $\epsilon=1/\tau_1$ and introducing the long time scale $T_1=\epsilon T_0$ with $T_0=\tau$. The analysis is carried out in exactly the same manner as before. The result is that the amplitudes $A_{q=1}$, $B_{q=1}$ are *exactly* given by Eq. (5.26). Furthermore, a consistency condition arising from the multitime scale analysis is that

$$A=4\sqrt{c_1^2+c_2^2}\approx 4c_2. \tag{5.32}$$

This condition is well verified in the numerical calculations.

Since the effective squared mass vanishes asymptotically and there are no resonances at $q=0$ for sufficiently late times, the $q=0$ mode behaves as

$$\varphi_0(\tau)=L+M\tau \tag{5.33}$$

where L and M are complex coefficients that can only be obtained from the full time evolution. The Wronskian relation (3.6) implies that

$$\mathrm{Im}[LM^*]=1, \tag{5.34}$$

showing that $M\neq 0\neq L$.

It follows from Eq. (3.8) that the number of $q=0$ quanta grows as τ^2 for asymptotically large τ:

$$N_0(\tau)\overset{\tau\to\infty}{=}\frac{1}{4}\sqrt{1+\eta_0^2}|M|^2\tau^2. \tag{5.35}$$

Notice that the total number of particles tends to a constant for $\tau\to\infty$ because $N_0(\tau)$ does not contribute to the total due to the vanishing of the phase space factor as q^2 at low momentum. This linear growth of the homogeneous quantum mode was also noticed in [34].

This situation is similar to Bose-Einstein condensation, in which case the excess number of particles at a fixed temperature goes into the condensate, whereas the total number of particles outside the condensate is fixed by the temperature at zero chemical potential. The $q=0$ mode does not contribute to the energy, the pressure and the total particle number but it will become macroscopically occupied for $\tau\approx\sqrt{V}$ with V the volume of the system, in which case the number of particles in the zero momentum mode becomes of the order of the spatial volume. In this case this mode must be isolated and studied separately from the $q\neq 0$ modes because its contribution to the momentum integral will be canceled by the small phase space at small momentum much the same way as in usual Bose-Einstein condensation.

The presence of a Bose condensate through this macroscopic zero momentum mode signals spontaneous symmetry breaking even when the order parameter remains zero. Therefore we identify the *linear growth* in time of the $q=0$ mode as the onset of a novel form of Bose condensation of Goldstone bosons and symmetry breaking in the collisionless regime and in the absence of thermalization. This form of Bose condensation of Goldstone bosons in a collisionless regime is similar to that reported recently within a different context [38].

The time scale for the formation of the condensate ($\tau\approx\sqrt{V}$) is obviously much larger than the nonlinear scale t_1 and the thermalization scale when corrections of order $1/N$ are included. Therefore, the formation of the Bose condensate including $1/N$ corrections, which will include collisions, will require a further understanding of the dynamics and of the time scales involved.

E. Energy and pressure for broken symmetry: Sum rules

As shown in Refs. [20,27] the energy (4.63) and the pressure (4.65) can be rewritten for broken symmetry as follows:

$$E_{ren}=\frac{2|M_R|^4}{\lambda_R}\varepsilon,$$

$$\varepsilon=\frac{\dot{\eta}^2}{2}+\frac{1}{4}(\eta^2-1)^2+2g\int_0^{q_u}q^2dq\Omega_q N_q(\tau)+\frac{g}{2}\Sigma(\tau)\left[-1-\eta_0^2+\mathcal{M}^2(\tau)-\frac{g}{2}\Sigma(\tau)\right]+\mathcal{O}(g),$$

$$P_{ren}(\tau)=\frac{2|M_R|^4}{\lambda_R}p(\tau), \tag{5.36}$$

$$p(\tau)=g\int_0^1 q^2dq\left[\frac{q^2}{3}|\varphi_q(\tau)|^2+|\dot{\varphi}(\tau)|^2\right]+\dot{\eta}^2+\mathcal{O}(g)-\varepsilon, \tag{5.37}$$

up to corrections of order $\eta_0^2\ll 1$ where q_u is the maximum spinodally unstable wave vector (for $\eta_0^2\ll 1 q_u=1$).

As for the unbroken symmetry case, we can use the asymptotic value of the effective mass squared and the conservation of the energy to compute the first two moments of $M_q^2(\infty)$ and to establish similar sum rules.

The vanishing of $\mathcal{M}^2(\infty)$ implies that $g\Sigma(\infty)=1+\mathcal{O}(\eta_0^2)$ and hence

$$\int_0^1 q^2dqM_q^2(\infty)+\mathcal{O}(g,\eta_0^2)=1, \tag{5.38}$$

where we used Eqs. (3.7) and (5.22).

Furthermore, equating the expression for the energy at $\tau=\infty$ [Eq. (5.36)] with its initial value

$$\varepsilon=\frac{1}{4}+\mathcal{O}(\eta_0^2) \tag{5.39}$$

yields the second sum rule

$$\int_0^1 q^4dqM_q^2(\infty)=\frac{1}{4}+\mathcal{O}(g,\eta_0^2). \tag{5.40}$$

Using these sum rules allows us to compute the pressure in the $\tau\to\infty$ limit from Eq. (5.36):

$$p(\infty)=\frac{1}{12}+\mathcal{O}(g,\eta_0^2), \tag{5.41}$$

leading to the equation of state for radiation,

$$p(\infty)=\frac{1}{3}\varepsilon+\mathcal{O}(g,\eta_0^2), \tag{5.42}$$

as is expected since the bulk of the produced particles are massless.

VI. CONCLUSIONS AND FURTHER QUESTIONS

In this article we have studied both numerically and analytically the asymptotic non-equilibrium dynamics of relaxation in a scalar field theory in the collisionless regime. We have focused on the relaxation of initial states of very large energy density that require a non-perturbative treatment in a controlled manner, maintaining renormalizability, energy conservation and all of the relevant conservation laws. Detailed numerical analysis revealed the presence of new dynamical and non-perturbative time scales and non-linear resonant bands that result in the power law growth of quantum fluctuations and a power law of relaxation for the expectation value of the scalar field. A separation between the time scales for weak coupling allowed us to implement a dynamical renormalization group resummation of secular terms via the method of multi-time scales and confirmed and completed the numerical results.

This *dynamical* renormalization group resummation of secular terms leads to power law relaxation with *anomalous* dynamical exponents which are *non-universal* depending non-perturbatively on the coupling constant.

In the unbroken symmetry phase the expectation value

vanishes asymptotically, transferring all of the initial energy into production of massive particles, as a result of the non-linear resonances and despite the presence of perturbative thresholds to particle production. The asymptotic distribution is non-thermal and non-perturbative in the band where parametric resonance takes place at early times. It can be interpreted as a ''semiclassical condensate'' in the unbroken phase, a result of the relaxation of the initial energy density. The equation of state of the produced particles interpolates between dust and radiation domination as a function of the initial amplitude of the expectation value of the scalar field.

In the broken phase the numerical evolution revealed a hierarchy of time scales, and the relaxation of the order parameter is with anomalous power laws. Again an implementation of the dynamical renormalization group revealed the presence of non-linear resonances that result in particle production after the spinodal time. Non-universal power law relaxation appears with exponents depending non-perturbatively on the coupling constant. The coupling constant dependence is similar for the unbroken and broken symmetry cases. The asymptotic distribution of particles is localized at low momenta and is non-perturbative and non-thermal, but the equation of state is that of radiation. We also found the onset of a novel form of Bose condensation in the collisionless regime and without thermalization but with extremely long time scales.

Although this body of results provides for a deeper understanding of the non-equilibrium dynamics in the collisionless regime, and thus we believe it represents a quantum field theory example of *non-linear dynamics*, there are very many unanswered questions that deserve further study: (i) The fact that the asymptotic distributions are of ''soft'' momenta and semiclassical in the sense that the amplitude of the particle distribution inside the bands is $\propto 1/\lambda$, and that there is a separation of time scales for weak coupling should allow a ''coarse grained'' description in terms of quasi-particle distributions in the manner of Boltzmann. (ii) The next order in $1/N$ must be pursued to incorporate consistently collisional processes; probably (i) must be understood before this to separate the microscopic from the long time scales. Collisions will compete with the collisionless processes and affect the onset of Bose condensation found in the collisionless regime. Here there is the possibility that whereas thermal equilibrium is established on collisional time scales, chemical equilibrium may be established on much longer time scales, resulting in a non-vanishing chemical potential.

Only a deeper understanding of (i) and (ii) will lead to a complete understanding of the different regimes, collisionless, kinetic and hydrodynamic, which could account for thermalization, chemical equilibration and all of the important relaxational phenomena.

ACKNOWLEDGMENTS

The authors thank F. Cooper, I. Egusquiza, H. J. Giacomini, E. Mottola and L. Yaffe, for stimulating discussions. D.B. thanks the NSF for partial support through grants PHY-9605186 and LPTHE for warm hospitality. R.H. is supported by DOE grant DE-FG02-91-ER40682. We thank NATO for partial support. LPTHE is Laboratoire Associé au CNRS VA280.

[1] L. P. Csernai, *Introduction to Relativistic Heavy Ion Collisions* (Wiley, England, 1994).

[2] C. Y. Wong, *Introduction to High-Energy Heavy Ion Collisions* (World Scientific, Singapore, 1994).

[3] J. W. Harris and B. Muller, Annu. Rev. Nucl. Part. Sci. **46**, 71 (1996); B. Muller in *Particle Production in Highly Excited Matter*, edited by H. H. Gutbrod and J. Rafelski (NATO Advanced Study Institute, Series B: Physics, Vol. 303) (Plenum, New York, 1993); B. Muller, *The Physics of the Quark Gluon Plasma* Lecture Notes in Physics Vol. 225 (Springer-Verlag, Berlin, 1985).

[4] J.-e. Alam, S. Raha, and B. Sinha, Phys. Rep. **273**, 243 (1996).

[5] H. Meyer-Ortmanns, Rev. Mod. Phys. **68**, 473 (1996).

[6] X. N. Wang and M. Gyulassy, Phys. Rev. D **44**, 3501 (1991); **45**, 844 (1992).

[7] K. Geiger and B. Muller, Nucl. Phys. **B369**, 600 (1992).

[8] K. Geiger, Phys. Rep. **258**, 237 (1995); Phys. Rev. D **46**, 4965 (1992); **47**, 133 (1993); in *Quark Gluon Plasma 2*, edited by R. C. Hwa (World Scientific, Singapore, 1995).

[9] H.-T. Elze and U. Heinz, in *Quark Gluon Plasma*, edited by R. C. Hwa (World Scientific, Singapore, 1990), and references therein.

[10] X.-N. Wang, in *Quark Gluon Plasma 2* [8].

[11] S. Mrowczynski, in *Quark Gluon Plasma* [9], and references therein.

[12] M. Gyulassy, *Quark Gluon Plasma* [9], and references therein.

[13] P. Danielewicz, Ann. Phys. (N.Y.) **152**, 239 (1984); St. Mrowczynski and P. Danielewicz, Nucl. Phys. **B342**, 345 (1990).

[14] E. M. Lifshitz and L. P. Pitaevskii, *Physical Kinetics* (Pergamon, New York, 1981).

[15] J. P. Blaizot, J. Y. Ollitrault and E. Iancu, *Quark Gluon Plasma* [8]; J.-P. Blaizot, in Proceedings of the Fourth Summer School and Symposium on Nuclear Physics, 1991, edited by D. P. Min and M. Rho (unpublished).

[16] H. A. Weldon, Phys. Rev. D **28**, 2007 (1983); Ann. Phys. (N.Y.) **228**, 43 (1993).

[17] Y. Kluger, J. M. Eisenberg, B. Svetitsky, F. Cooper, and E. Mottola, Phys. Rev. Lett. **67**, 2427 (1991); Phys. Rev. D **45**, 4659 (1992); **48**, 190 (1993); F. Cooper, in *Particle Production in Highly Excited Matter* [3]; F. Cooper and E. Mottola, Mod. Phys. Lett. A **2**, 635 (1987); F. Cooper, S. Habib, Y. Kluger, E. Mottola, J. P. Paz, and P. R. Anderson, Phys. Rev. D **50**, 2848 (1994); F. Cooper, S.-Y. Pi, and P. N. Stancioff, *ibid.* **34**, 3831 (1986); F. Cooper, Y. Kluger, E. Mottola, and J. P. Paz, *ibid.* **51**, 2377 (1995); F. Cooper and E. Mottola, *ibid.* **36**, 3114 (1987); Y. Kluger, F. Cooper, E. Mottola, J. P. Paz, and A. Kovner, Nucl. Phys. **A590**, 581c (1995); M. A. Lampert, J. F. Dawson, and F. Cooper, Phys. Rev. D **54**, 2213 (1996); F. Cooper, Y. Kluger, and E. Mottola, Phys. Rev. C **54**, 3298 (1996).

[18] D. Boyanovsky and H. J. de Vega, Phys. Rev. D **47**, 2343 (1993); D. Boyanovsky, D.-S. Lee, and A. Singh, *ibid.* **48**, 800 (1993); D. Boyanovsky, H. J. de Vega, and R. Holman, *ibid.* **51**, 734 (1995).

[19] J. Traschen and R. Brandenberger, Phys. Rev. D **42**, 2491 (1990); Y. Shtanov, J. Traschen, and R. Brandenberger, *ibid.* **51**, 5438 (1995); L. Kofman, A. Linde, and A. Starobinsky, Phys. Rev. Lett. **73**, 3195 (1994); **76**, 1011 (1996); L. Kofman, astro-ph/9605155 (1996); S. Yu. Khlebnikov and I. I. Tkachev, Phys. Rev. Lett. **77**, 219 (1996); Phys. Lett. B **390**, 80 (1997); D. T. Son, Phys. Rev. D **54**, 3745 (1996); hep-ph/9601377; I. I. Tkachev, Phys. Lett. B **376**, 35 (1996); A. Riotto and I. I. Tkachev, *ibid.* **385**, 57 (1996); E. W. Kolb and A. Riotto, Phys. Rev. D **55**, 3313 (1997); D. I. Kaiser, *ibid.* **53**, 1776 (1996); **57**, 702 (1998); **56**, 706 (1997); H. Fujisaki, K. Kumekawa, M. Yamaguchi, and M. Yoshimura, Phys. Rev. D **53**, 6805 (1996); M. Yoshimura, Prog. Theor. Phys. **94**, 873 (1995); hep-ph/9605246 (1996); H. Fujisaki, K. Kumekawa, M. Yamaguchi, and M. Yoshimura, Phys. Rev. D **53**, 6805 (1996); **54**, 2494 (1996); S. Kasuya and M. Kawasaki, Phys. Lett. B **388**, 686 (1996).

[20] D. Boyanovsky, H. J. de Vega and R. Holman, in *Proceedings of the Second Paris Cosmology Colloquium*, Observatoire de Paris, 1994, edited by H. J. de Vega and N. Sanchez (World Scientific, Singapore, 1995), pp. 127–215; in *Advances in Astrofundamental Physics*, Erice Chalonge Course, edited by N. Sanchez and A. Zichichi (World Scientific, Singapore, 1995); D. Boyanovsky, H. J. de Vega, R. Holman, D.-S. Lee, and A. Singh, Phys. Rev. D **51**, 4419 (1995); D. Boyanovsky, H. J. de Vega, R. Holman, and J. Salgado, *ibid.* **54**, 7570 (1996).

[21] S. A. Ramsey, B. L. Hu, and A. M. Stylianopoulos, Phys. Rev. D (to be published), hep-ph/9709267; S. A. Ramsey and B. L. Hu, Phys. Rev. D **56**, 678 (1997); **56**, 661 (1997).

[22] I. Zlatev, G. Huey, and P. J. Steinhardt, astro-ph/9709006.

[23] D. Boyanovsky, D. Cormier, H. J. de Vega, and R. Holman, Phys. Rev. D **55**, 3373 (1997); D. Boyanovsky, D. Cormier, H. J. de Vega, R. Holman, A. Singh, and M. Srednicki, *ibid.* **56**, 1939 (1997); D. Boyanovsky, D. Cormier, H. J. de Vega, R. Holman, and S. P. Kumar, astro-ph/9707267; Phys. Rev. D **57**, 2166 (1998); D. Boyanovsky, D. Cormier, H. J. de Vega, and R. Holman, *ibid.* **55**, 3373 (1997).

[24] D. Boyanovsky, M. D'Attanasio, H. J. de Vega, and R. Holman, Phys. Rev. D **54**, 1748 (1996).

[25] For a thorough exposition of non-equilibrium methods in cosmology see, for example, E. Calzetta and B.-L. Hu, Phys. Rev. D **35**, 495 (1988); **37**, 2838 (1988); J. P. Paz, *ibid.* **41**, 1054 (1990); **42**, 529 (1990); B.-L. Hu, in *Bannf/Cap Workshop on Thermal Field Theories: Proceedings*, edited by F. C. Khanna, R. Kobes, G. Kunstatter, and H. Umezawa (World Scientific, Singapore, 1994), p. 309; in *Proceedings of the Second Paris Cosmology Colloquium*, Observatoire de Paris, edited by H. J. de Vega and N. Sánchez (World Scientific, Singapore, 1995), p. 111, and references therein.

[26] J. Schwinger, J. Math. Phys. **2**, 407 (1961); P. M. Bakshi and K. T. Mahanthappa, *ibid.* **4**, 1 (1963); **4**, 12 (1963); L. V. Keldysh, Sov. Phys. JETP **20**, 1018 (1965); A. Niemi and G. Semenoff, Ann. Phys. (N.Y.) **152**, 105 (1984); Nucl. Phys. **B230**, 181 (1984); E. Calzetta, Ann. Phys. (N.Y.) **190**, 32 (1989); R. D. Jordan, Phys. Rev. D **33**, 444 (1986); N. P. Landsman and C. G. van Weert, Phys. Rep. **145**, 141 (1987); R. L. Kobes and K. L. Kowalski, Phys. Rev. D **34**, 513 (1986); R. L. Kobes, G. W. Semenoff, and N. Weiss, Z. Phys. C **29**, 371 (1985).

[27] D. Boyanovsky, H. J. de Vega and R. Holman, in *Proceedings of the Vth Erice School ''D. Chalonge,''* Current Topics in Astrofundamental Physics, edited by N. Sánchez and A. Zichichi (World Scientific, Singapore, 1997), pp. 183–270.

[28] A. Nayfeh, *Perturbation Methods* (Wiley, New York, 1973); A. Nayfeh and D. T. Mook, *Nonlinear Oscillations* (Wiley, New York, 1979).

[29] H. J. de Vega and J. F. J. Salgado, Phys. Rev. D **56**, 6524 (1997), and references therein.

[30] C. M. Bender and L. M. A. Bettencourt, Phys. Rev. D **54**, 7710 (1996); Phys. Rev. Lett. **77**, 4114 (1996), and references therein.

[31] I. L. Equsquiza and M. A. Valle-Basagoiti, hep-th/9611143.

[32] I. S. Gradshteyn and I. M. Ryshik, *Table of Integrals, Series and Products* (Academic, New York, 1980).

[33] J. Baacke, K. Heitmann, and C. Patzold, hep-ph/970627; Phys. Rev. D **55**, 2320 (1997).

[34] F. Cooper, S. Habib, Y. Kluger, and E. Mottola, Phys. Rev. D **55**, 6471 (1997).

[35] D. Boyanovsky, D. Cormier, H. J. de Vega, and R. Holman, Phys. Rev. D **55**, 3373 (1997).

[36] D. Boyanovsky, D. Cormier, H. J. de Vega, R. Holman, A. Singh, and M. Srednicki, Phys. Rev. D **56**, 1939 (1997).

[37] D. Boyanovsky, D. Cormier, H. J. de Vega, R. Holman, and S. P. Kumar, astro-ph/9707267.

[38] D. Boyanovsky, H. J. de Vega, S. P. Kumar, R. Holman, and R. D. Pisarski, Phys. Rev. D (to be published), hep-ph/9711258.